U.S. DEPARTMENT OF COMMERCE
National Technical Information Service
PB80-122252

Dust Transport in Maricopa County, Arizona

Texas Univ at Austin Dept of Chemical Engineering

Prepared for

Environmental Sciences Research Lab, Research Triangle Park, NC

Sep 79

PB80-122252

United States
Environmental Protection
Agency

Environmental Sciences Research
Laboratory
Research Triangle Park NC 27711

EPA-600/3-79-082
September 1979

Research and Development

EPA

Dust Transport in Maricopa County, Arizona

REPRODUCED BY
NATIONAL TECHNICAL
INFORMATION SERVICE
U. S. DEPARTMENT OF COMMERCE
SPRINGFIELD, VA. 22161

TECHNICAL REPORT DATA
(Please read Instructions on the reverse before completing)

1. REPORT NO.	2.	3. RECIPIENT'S ACCESSION NO.
EPA-600/3-79-082		PB 80 122252

4. TITLE AND SUBTITLE	5. REPORT DATE
DUST TRANSPORT IN MARICOPA COUNTY, ARIZONA	September 1979
	6. PERFORMING ORGANIZATION CODE

7. AUTHOR(S)	8. PERFORMING ORGANIZATION REPORT NO.
S. Suck, E. Upchurch and J. Brock	

9. PERFORMING ORGANIZATION NAME AND ADDRESS	10. PROGRAM ELEMENT NO.
University of Texas Department of Chemical Engineering Austin, Texas 78712	1AA603 AE-09 (FY-77)
	11. CONTRACT/GRANT NO.
	803660

12. SPONSORING AGENCY NAME AND ADDRESS	13. TYPE OF REPORT AND PERIOD COVERED
Environmental Sciences Research Laboratory - RTP, NC Office of Research and Development U.S. Environmental Protection Agency Research Triangle Park, North Carolina 27711	Final 12-75 - 12/77
	14. SPONSORING AGENCY CODE
	EPA/600/09

15. SUPPLEMENTARY NOTES

16. ABSTRACT

Numerical simulations have been carried out for ambient air, supermicrometric particulate concentrations in Maricopa County, Arizona during late fall and winter periods of atmospheric stability. Results of model studies are in approximate agreement with limited field observational data. On the basis of the model studies, observed high particulate concentrations in Maricopa County urban areas during late fall and winter periods of atmospheric stability are associated with local fugitive dust sources. Because of light drainage winds prevalent during these periods, advective transport of dust from countryside to the urban areas is not an important contribution to urban supermicrometeric particulate concentrations. Surface roughness, dry deposition, and source strengths are among the most important determinants of ground level concentrations. Reduction in ground level concentrations could be effected through control of dust emissions, as well as by planting trees and other foliage to increase surface roughness and particle deposition. An adequate and practical predictive model, along the lines of the current model, could be developed for Maricopa County as well as for other urban areas in high desert regions.

17. KEY WORDS AND DOCUMENT ANALYSIS

a. DESCRIPTORS	b. IDENTIFIERS/OPEN ENDED TERMS	c. COSATI Field/Group
*Air pollution *Dust *Sources *Atmospheric circulation *Mathematical models *Surface roughness	Maricopa County, Arizona	13B 11G 04B 12A

18. DISTRIBUTION STATEMENT	19. SECURITY CLASS *(This Report)*	21. NO. OF PAGES
RELEASE TO PUBLIC	UNCLASSIFIED	51
	20. SECURITY CLASS *(This page)*	22. PRICE
	UNCLASSIFIED	

EPA Form 2220-1 (9-73)

EPA-600/3-79-082
September 1979

DUST TRANSPORT IN MARICOPA COUNTY, ARIZONA

by

S. Suck, E. Upchurch, and J. Brock
University of Texas
Austin, Texas 78712

Grant No. 803660

Project Officer

Jack L. Durham
Atmospheric Chemistry and Physics Division
Environmental Sciences Research Laboratory
Research Triangle Park, North Carolina 27711

ENVIRONMENTAL SCIENCES RESEARCH LABORATORY
OFFICE OF RESEARCH AND DEVELOPMENT
U.S. ENVIRONMENTAL PROTECTION AGENCY
RESEARCH TRIANGLE PARK, NORTH CAROLINA 27711

DISCLAIMER

This report has been reviewed by the Environmental Sciences Research Laboratory, U.S. Environmental Protection Agency, and approved for publication. Approval does not signify that the contents necessarily reflect the views and policies of the U.S. Environmental Protection Agency, nor does mention of trade names or commercial products constitute endorsement or recommendation for use.

ABSTRACT

Numerical simulations have been carried out for ambient supermicrometric particulate concentrations in Maricopa County, Arizona during late fall and winter periods of atmospheric stability. Results of model studies are in approximate agreement with limited field observational data. On the basis of the model studies it is concluded that observed high particulate concentrations in Maricopa County urban areas during late fall and winter periods of atmospheric stability are associated with local fugitive dust sources. Because of light drainage winds prevalent during these periods, advective transport of dust from countryside to the urban areas is not an important contribution to urban supermicrometric particulate concentrations. Surface roughness, dry deposition, and source strengths, are among the most important determinants of ground level concentrations. Reduction in ground level concentrations could be effected through control of dust emissions, as well as by planting trees and other foliage to increase surface roughness and particle deposition. An adequate and practical predictive model, along the lines of the current model, could be developed for Maricopa County as well as for the other urban areas in the high desert regions.

This report was submitted in fulfillment of Grant R803660 by the University of Texas, Austin under the sponsorship of the U.S. Environmental Protection Agency. This report covers a period from December 1, 1975 to December 1, 1977, and work was completed as of March 1, 1978.

CONTENTS

Abstract iii
Figures vii
Tables viii

1. Introduction 1
2. Procedure. 2
3. Data for Modelling Maricopa Co. 5
4. Results. 11
5. Conclusions 40

References 41

Preceding page blank

FIGURES

Number		Page
1	Study area in Maricopa Co., Arizona with day wind field of Berman and Delaney (10)	6
2	Study area in Maricopa Co., Arizona with day wind field of Berman and Delaney (10)	7
3	Estimated variation with time of traffic dust.	9
4	Dust concentration at 10m for Maricopa County, Arizona, UTM Easting 358ooo to 446ooo, UTM Northing 3670ooo to 3734ooo.	12
5	Dust concentration at 10m for Maricopa County, Arizona, UTM Easting 358ooo to 446ooo, UTM Northing 3670ooo to 3734ooo.	13
6	Dust concentration at 10m for Maricopa County, Arizona, UTM Easting 358ooo to 446ooo, UTM Northing 3670ooo to 3734ooo.	14
7	Dust concentration at 10m for Maricopa County, Arizona, UTM Easting 358ooo to 446ooo, UTM Northing 3670ooo to 3734ooo.	15
8	Dust concentration at 10m for Maricopa County, Arizona, UTM Easting 358ooo to 446ooo, UTM Northing 3670ooo to 3734ooo.	16
9	Dust concentration at 10m for Maricopa County, Arizona, UTM Easting 358ooo to 446ooo, UTM Northing 3670ooo to 3734ooo.	17
10	Dust concentration at 10m for Maricopa County, Arizona, UTM Easting 358ooo to 446ooo, UTM Northing 3670ooo to 3734ooo.	18
11	Dust concentration at 10m for Maricopa County, Arizona, UTM Easting 358ooo to 446ooo, UTM Northing 3670ooo to 3734ooo.	19

Number		Page
12	Particle concentration isopleths in $\mu g/m^3$ in plane perpendicular to surface at UTM Northing 3702ooo extending from UTM Easting 382ooo to 422ooo.	32
13	Particle concentration isopleths in $\mu g/m^3$ in plane perpendicular to surface at UTM Northing 3702ooo extending from UTM Easting 382ooo to 422ooo.	33
14	Particle concentration isopleths in $\mu g/m^3$ in plane perpendicular to surface at UTM Northing 3702ooo extending from UTM Easting 382ooo to 422ooo.	34
15	Particle concentration isopleths in $\mu g/m^3$ in plane perpendicular to surface at UTM Northing 3702ooo extending from UTM Easting 382ooo to 422ooo.	35
16	Particle concentration isopleths in $\mu g/m^3$ in plane perpendicular to surface at UTM Northing 3702ooo extending from UTM Easting 382ooo to 422ooo.	36
17	Particle concentration isopleths in $\mu g/m^3$ in plane perpendicular to surface at UTM UTM Easting 398ooo extending from UTM Northing 3694ooo to 3734ooo	37

TABLES

Number		Page
1	Calculated Hourly Particulate Concentrations ($\mu g/m^3$) at 10 Meters above the Surface. (See Fig. 4)	20
2	Calculated Hourly Particulate Concentrations ($\mu g/m^3$) at 10 Meters above the Surface. (See Fig. 6)	24

SECTION 1

INTRODUCTION

Many urban areas in the high desert regions of the western United States consistently exceed the national ambient air quality standards for particulate matter. In considering control strategies for these areas, complex predictive models of suspended particulate matter dynamics are necessary. Empirical models, which correlate limited observational data, are ineffective in examining and predicting alternative control strategies.

High ambient particulate concentrations (as measured by high-volume samplers) are usually observed in Maricopa, Co. during late fall and winter days. During this period, meteorological conditions are characterized by light drainage winds associated with the area's valley topography. The whole area forms an air drainage basin with a gentle slope down the area's rivers from east to west. The analysis, presented here covers typical drainage and other conditions prevalent during late November in Maricopa Co.

A comprehensive computer code, AROSOL, was used to analyze the aerosol dynamics.

SECTION 2

PROCEDURE

Of all the atmospheric trace constituents, the atmospheric aerosol probably possesses the most complex dynamical features. These include such processes as coagulation, condensation, nucleation, sedimentation, deposition, resuspension, primary and secondary source inputs, and advection and dispersion.

The advent of high speed computers has made it feasible to deal with these complexities (1,2). Computer code AROSOL has been developed by us to investigate atmospheric aerosol dynamics. AROSOL gives a numerical solution of the following equation describing the evolution of the singlet density function of an aerosol.

$$\partial n(\mu;r,t)/\,t + \nabla \cdot Un(\mu;r,t) = (K_x + K_y)\nabla^2 n(\mu;r,t)$$

$$+ \nabla \cdot K_z(r,t)\nabla n(\mu;r,t) + 1/2 \int_0^{\mu} d\mu' b(\mu-\mu',\mu') n(\mu-\mu';r,t) n(\mu';r,t)$$

$$- n(\mu;r,t) \int_0^{\infty} d\mu b(\mu,\mu') n(\mu';r,t) - \frac{\partial}{\partial \mu} [\psi(\mu;r,t) n(\mu;r,t)]$$

$$+ G(\mu)\cdot\nabla n(\mu;r,t) + \sum_i \sigma_i + \sum_j \nu_j \qquad (1)$$

Boundary and initial conditions may be set as a particular physical system demands, but always includes phenomena such as dry deposition at boundary surfaces. $n(\mu;r,t)$ represents the number of aerosol particles having mass μ in the range $\mu,d\mu$ at a point in space r at time t. In the atmosphere, U is the time average wind speed. K_x, K_y, and K_z are the turbulent eddy diffusivities (a rectangular Eulerian coordinate system is employed) in the x,y, and z directions, respectively. The fourth and fifth terms on the right hand size of (1) account for particle coagulation. The sixth term

represents condensation, and the seventh graviational sedimentation, G being the sedimentation velocity. The last two terms allow for input of primary source aerosol, σ_i, and aerosol resulting from homogeneous nucleation of trave gaseous species, ν_j.

Eq. (1) is coupled to the corresponding onservation equations of those trace gaseous species which act as sources of secondary aerosol (3). The appropriateness of eq. (1) for representing the evolution of an aerosol under conditions of atmospheric turbulence has been verified (4,5).

The details of the numerical solution of eq. (1) and of computer time and memory requirements will be covered in another publication (6). The portion of AROSOL dealing with advection and dispersion is a modification of an earlier computer code due to Shir and Shieh (7).

In modelling particulate concentrations for Maricopa County during stable late fall periods, considerable simplification of eq. (1) is possible. Source emission data (8) and dichotomous and hi-vol data (9) show that supermicrometric dust is the largest contributor to the large (24 hour averages of 100-300 $\mu g/m^3$) ambient particulate concentrations. For this situation, coagulation, condensation, and nucleation all play negligible roles. Hence the following equation has been employed in our model:

$$\partial n(\mu;r,t)/\partial t + \nabla\cdot Un(\mu;r,t) = (K_x + K_y)\nabla^2 n(\mu;r,t)$$

$$+\nabla\cdot K_z \nabla n(\mu;r,t) + G\cdot\nabla n(\mu;r,t)$$

$$+\sum_i \sigma_i \qquad (2)$$

with boundary conditions:

$$\frac{\partial^2 n}{\partial x^2} = 0;\ x = 0,\ x = x_{max} \qquad (3)$$

$$\frac{\partial^2 n}{\partial y^2} = 0;\ y = 0,\ y = y_{max} \qquad (4)$$

$$nV_d = -(K_z + D(\mu))\frac{\partial n}{\partial z} - Gn;\ z = 0 \qquad (5)$$

$$\frac{\partial n}{\partial z} = 0;\ z = z_{max} \qquad (6)$$

$$n = n_o(\mu;r,t);\ t = 0 \qquad (7)$$

where z is the axis perpendicular to the surface at a point x,y of a grid covering Maricopa Co. In eq. (5), V_d is the deposition velocity; $G(\mu)$ the sedimentation velocity at the surface point x,y; and D the Brownian diffusion coefficient of particle of mass, μ.

SECTION 3

DATA FOR MODELLING MARICOPA CO.

Even with the simplifications introduced in arriving at eq. (2), the dynamical system is still very complex. Accurate modelling represents a large project in data processing. Data inputs comprise the following items:

(1) Numerical grid for a portion of Maricopa Co.

(2) Elevations for a portion of Maricopa Co.

(3) Particulate area and point source emissions data.

(4) Particle size distributions and diurnal variation of particulate emissions.

(5) Surface roughness.

(6) Wind data.

(7) Particulate dry deposition.

(8) Diurnal variation of mixing heights.

(9) Atmospheric dispersion coefficients.

These data inputs will be discussed in order.

(1) Numerical grid for a portion of Maricopa Co.: An area of 92 km. by 68 km. (see Figs. 1&2) was chosen for this analysis. A grid 23 x 17 consisting of 4 km. x 4 km. squares covers the area. These choices were determined by the available wind data of Berman and DeLaney (10).

(2) Elevations for a portion of Maricopa Co.: Elevations in meters were required for each grid square. These were estimated from a variety of sources (10,11,12).

(3) Particulate area and point source emissions data: These were estimated for each grid point from 1975 winter quarter data of TRW, Inc. (8).

(4) Particle size distributions and diurnal variations of particulate emissions: These were estimated as in a previous study of Denver pollution episodes (13). Three major categories of dust emissions were considered:

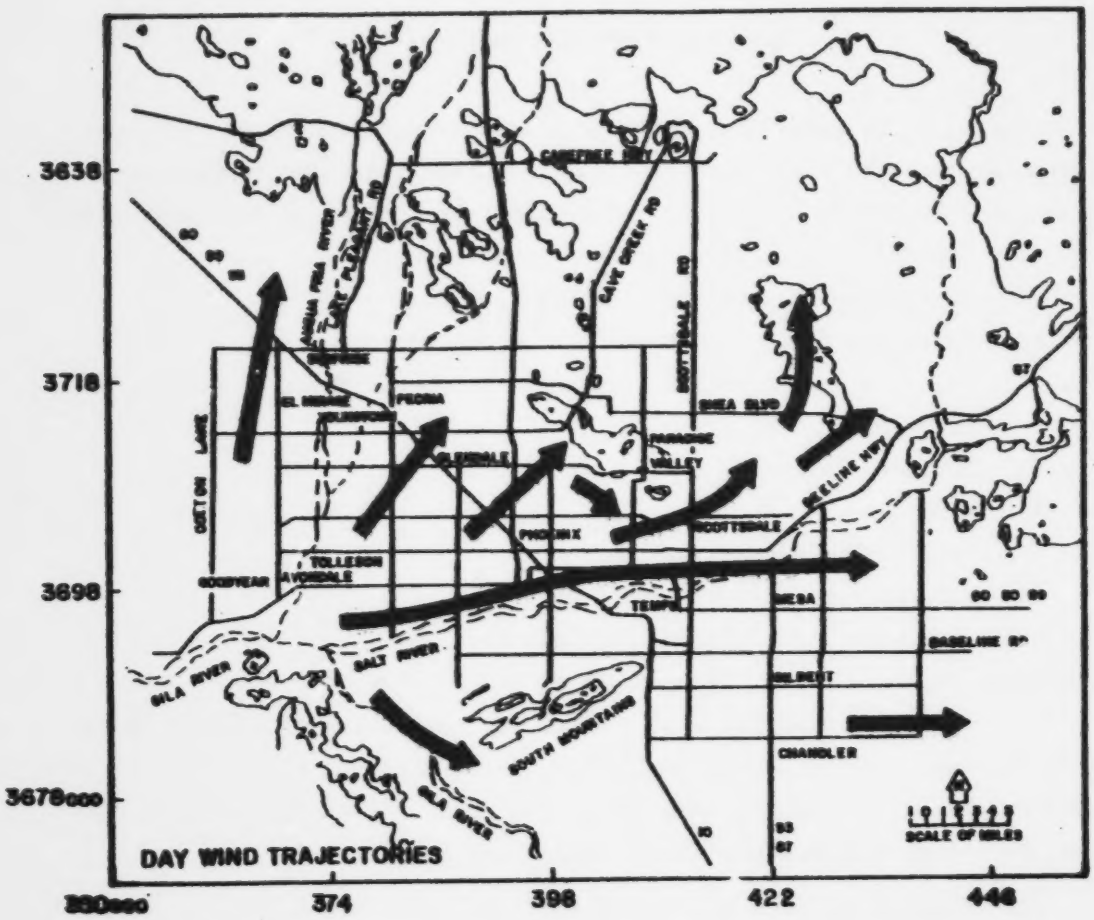

Figure 1. Study area in Maricopa Co., Arizona with day wind field of Berman and Delaney (10).

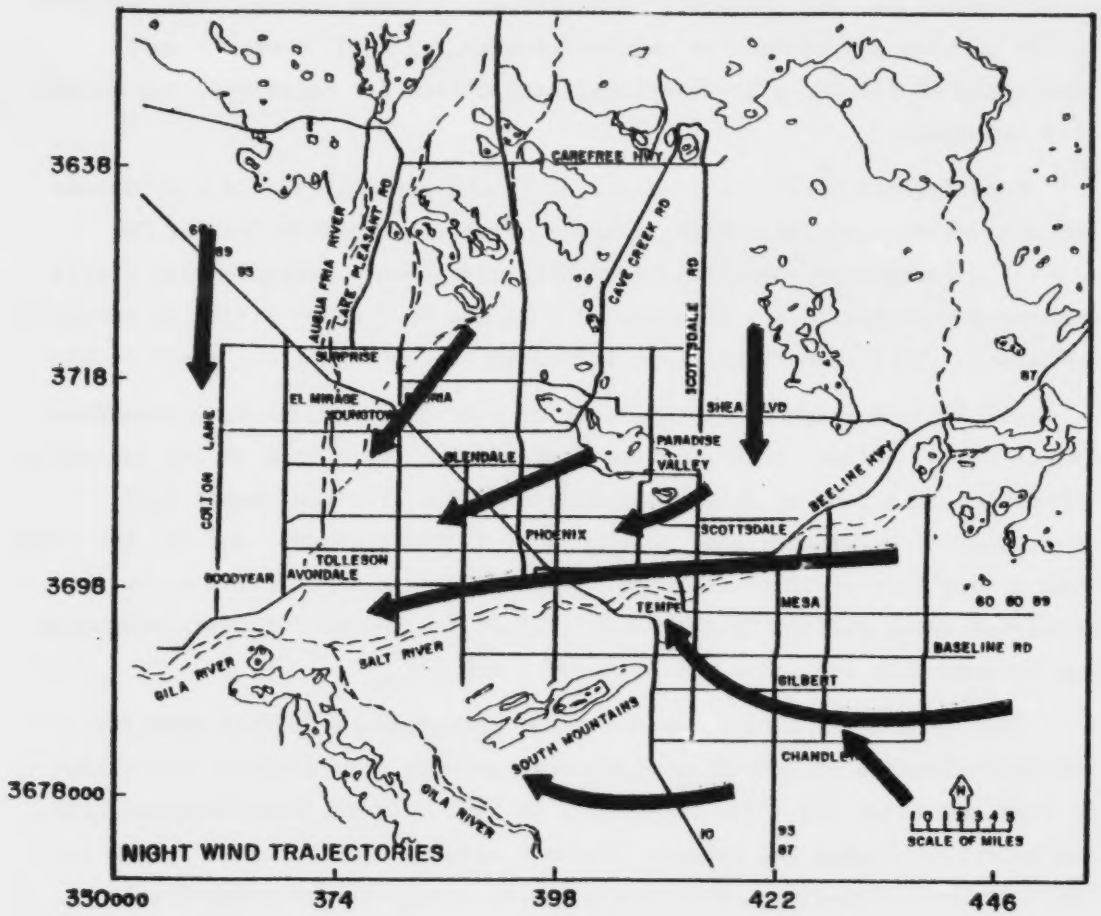

Figure 2. Study area in Maricopa Co., Arizona with day wind field of Berman and Delaney (10).

(a) "traffic dust" consisting of unpaved automotive roadway emissions, wind-blown unpaved roadway emissions, and off-roadway vehicle emissions. (Variation with time of this component is given in Fig. 3.) (b) "diurnal dust" consisting of agricultural tillage emissions, wind-blown undisturbed desert emissions, and construction emissions. (These sources were "switched on" at sunrise and thereafter remained constant.) (c) "constant dust" consisting of tailing pile emissions, cattle feed lot emissions, and vacant soil emissions.

Considerable uncertainty exists as to the particle size distributions for the various sources. Also, computer time requirements for the CDC 6400/6600 system for accurately including atmospheric particle size distributions are prohibitive. We assigned a single mean diameter to the suspended particles. This mean diameter is varied in the course of our model studies.

(5) Surface roughness: Two types of surface roughness were considered. "Micro-scale" surface roughness was required for estimation of dry deposition velocities from data of Sehmel and Hodgson (14). For the desert area (unpopulated) a "micro-scale" roughness of 3 cm was chosen, and for the urban area a roughness of 10 cm was used. The urban area was defined to be the populated areas defined by reference (12). "Macro-scale" surface roughness was estimated by the method of Shir and Shieh (7).

(6) Wind data: These include x and y components of wind velocity and determination of stability class from average wind speed by the method of Shir and Shieh (7). The components of wind velocity were obtained from the report of Berman and DeLaney (10) and adjusted for our grid system by the continuity equation. Wind trajectories are given schematically in Figs. 1 and 2.

(7) Particulate dry deposition: This input relates to the boundary condition of eq. (5). Deposition velocities, V_d, were calculated from the correlation of Sehmel and Hodgson (14) for a friction velocity of 10 cm/sec. Sedimentation velocities, G_z, were calculated by standard methods (15).

(8) Diurnal variation of mixing height, H: These were obtained for November 1974 from the daily mixing height studies of NOAA (16). The diurnal

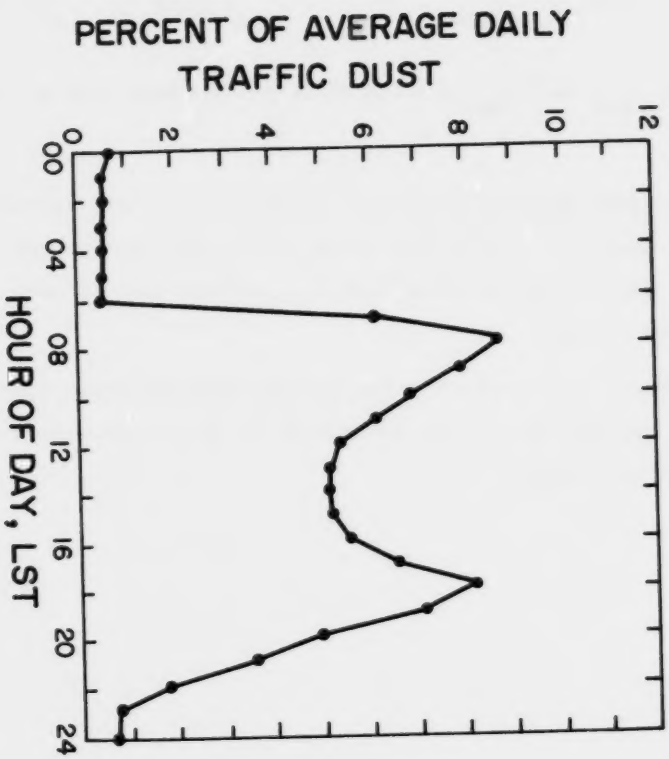

Figure 3. Estimated variation with Time of traffic dust.

variations during this period were as follows in LST:

$$0 - 0500,\ H = H_{min}$$

$$0600 - 1300,\ H = H_{min} + (H_{max} - H_{min})(\text{LST hr.} - 5.5)/8$$

$$1400 - 1800,\ H = H_{max}$$

$$1800 - 2400,\ H = H_{max} - (H_{max} - H_{min})\ (\text{LST hr.} - 17.5)/6$$

Typical values of H_{min} and H_{max} during this period were 130 m. and 1650 m., respectively.

(9) The vertical eddy diffusivity, $K_z(x, y, z)$, was calculated according to the methods of Shir and Shieh (7). The horizontal eddy diffusivity, K_H, was chosen as 10 m^2/sec to reflect the assumed stable meteorological conditions.

From these basic data inputs other parameters entering into eq. (2) and the boundary conditions can be estimated by known methods in the absence of actual field measurements. (7).

SECTION 4

RESULTS

GENERAL FEATURES

As is evident from the discussion in the previous section, data input requirements for eq. (2) are relatively large and, in the present study, were obtained from a wide variety of sources. An accurate case study would require at least hourly measurements of wind velocity as a function of altitude over the study area. More accurate and detailed particulate emissions data would also be necessary. Effects of "macroscale" roughness can be assessed through a study of distribution of an inert species. Validation of a case study would require accurate data (at least hourly) on particulate concentrations and particle size distributions as a function of altitude over the study area. Since none of these refined data souces were available to us, our approach is to present a model study in which the sensitivity of total ambient particulate concentrations to the various model parameters is examined. This study indicates the important dynamical features governing ambient particulate concentrations. Because of the complex interrelationships of the various processes in the model, the effects of varying one of the parameters are not intuitively obvious and are revealed only by such a model study as performed here.

For purposes of limited comparison with the IITRI Field Sampling Study (9) and with the high-vol data for the region (9), calculated hourly particulate concentrations at 10 meters above the surface are presented in Tables 1 and 2 and Figs. 4 to 11 with variation of mean particle size, wind speed, and dry deposition. Particle concentration isopleths are given in Figs. 12 to 17 in a cross section up to an altitude of 300m above surface and progressing from UTM Easting 382_{000} to 422_{000} at UTM Northing 3702_{000}. This cross section, runs from Tolleson on the west through the center of Phoenix and ends just north of Mesa.

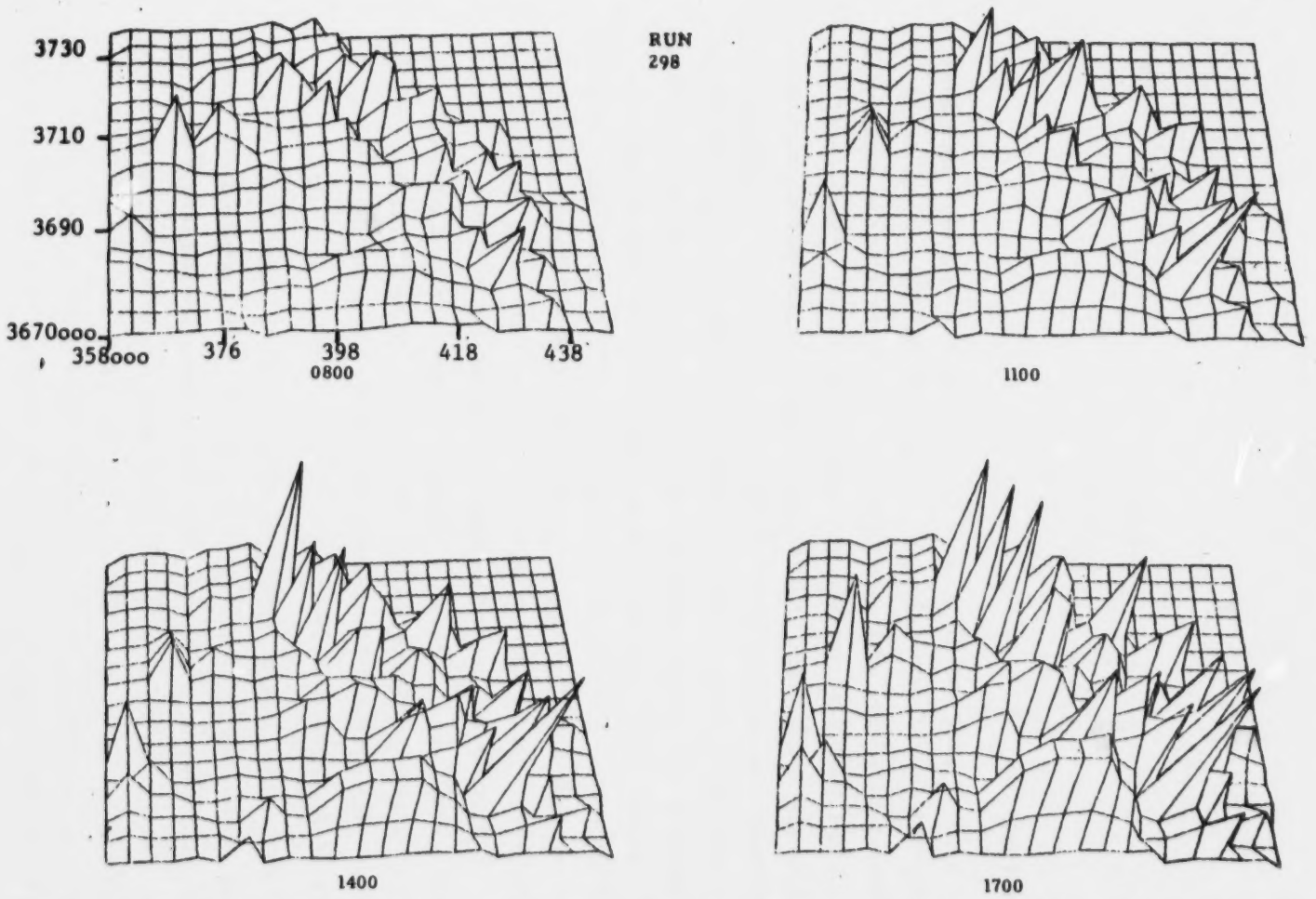

Figure 4. Dust Concentration at 10m for Maricopa County, Arizona, UTM Easting 358ooo to 446ooo, UTM Northing 3670ooo to 3734ooo.

Particle Size: 5 μm, Wind Field: 1X. Gravitational Sedimentation and Deposition Operating. Height above surface proportional to particle concentration in $\mu g/m^3$ (See Table 1).

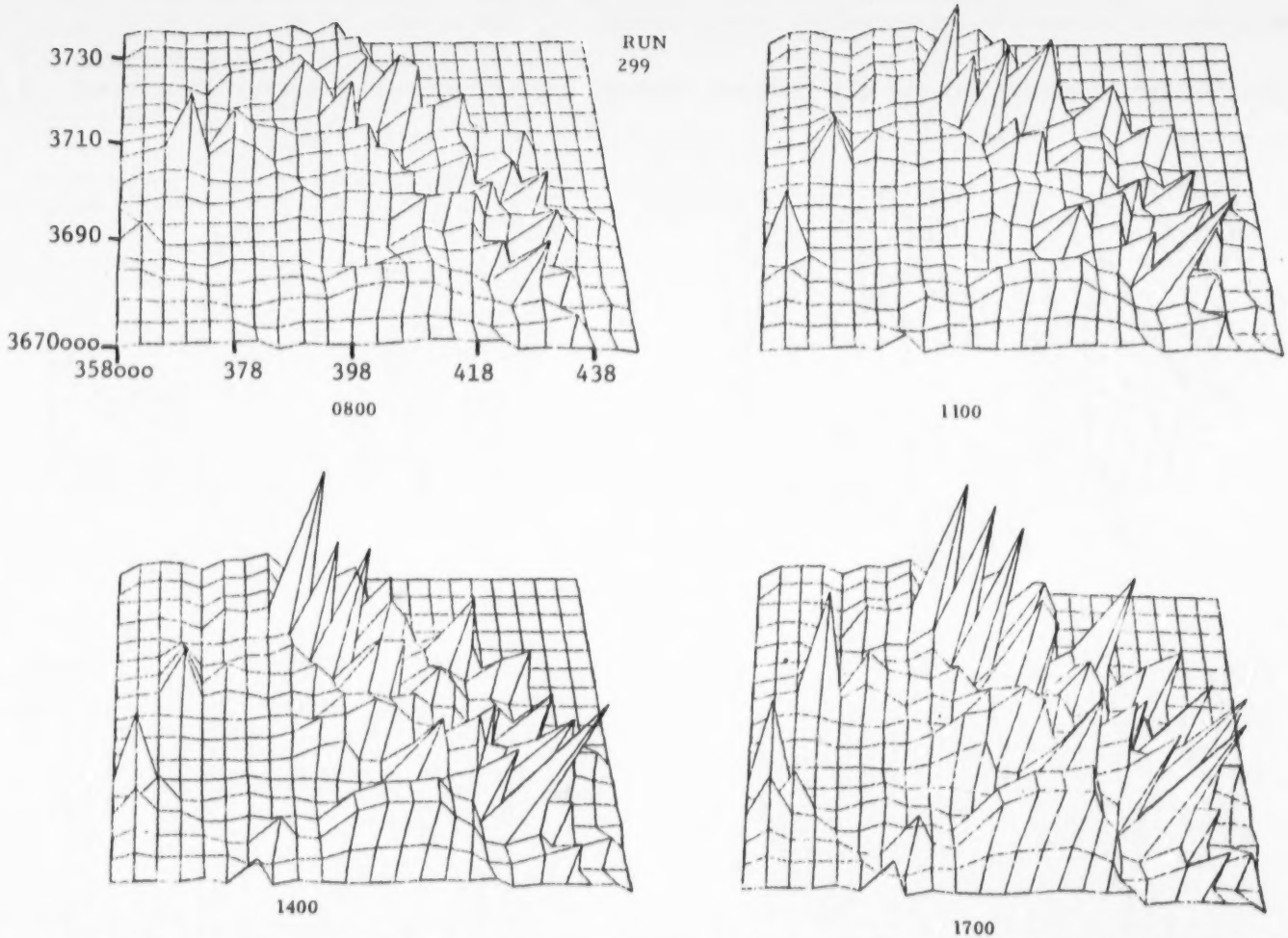

Figure 5. Dust Concentration at 10m for Maricopa County, Arizona, UTM Easting 358ooo to 446ooo, UTM Northing 3670ooo to 3734ooo.

Particle Size: 5 μm, Wind Field: 1X. Gravitational Sedimentation and Deposition Operating. Height above surface proportional to particle concentration in $\mu g/m^3$.

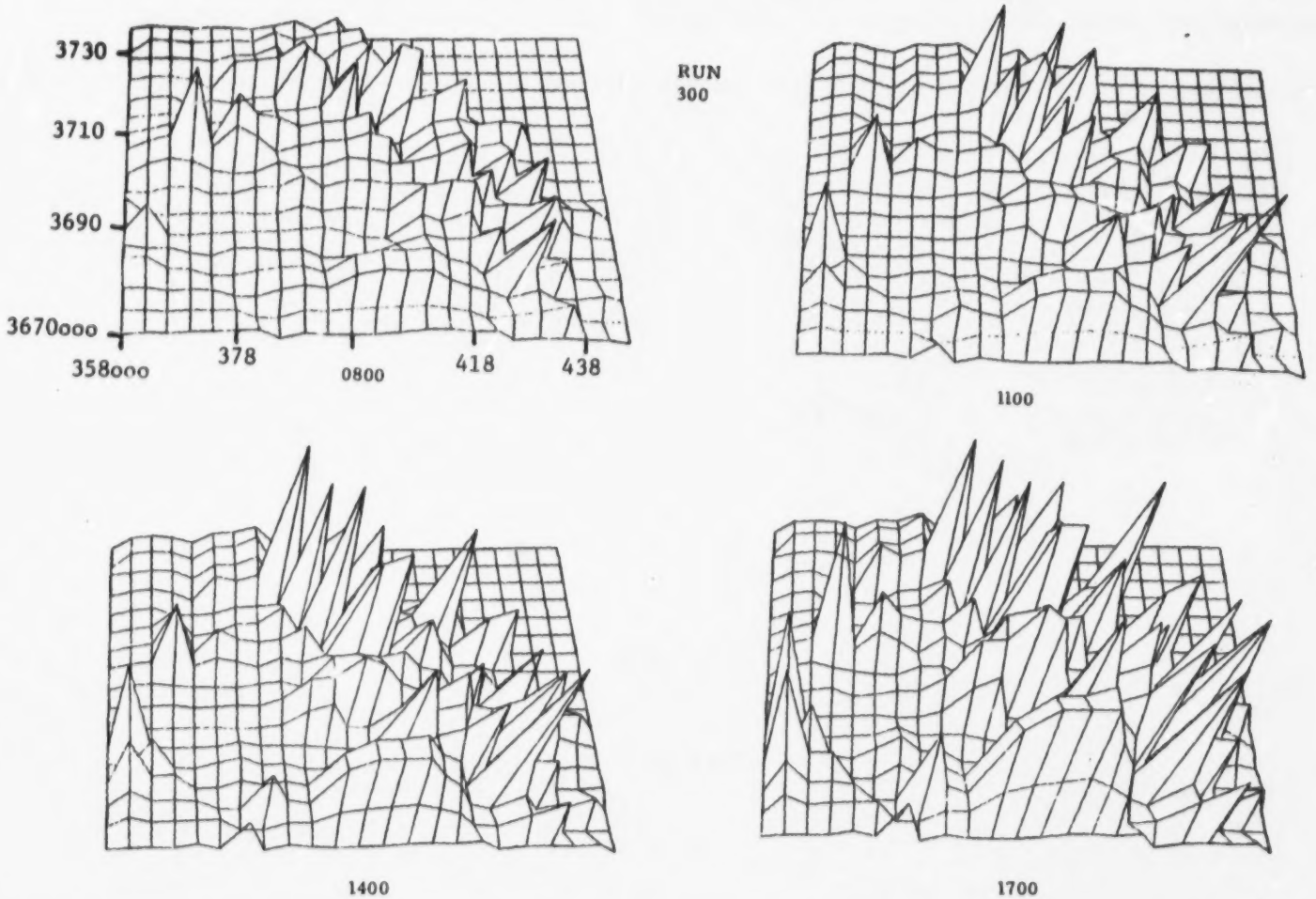

Figure 6. Dust Concentration at 10m for Maricopa County, Arizona, UTM Easting 358ooo to 446ooo, UTM Northing 3670ooo to 3734ooo.

Particle Size: 20 μm, Wind Field: 1X. Gravitational Sedimentation and Deposition Operating. Height above surface proportional to particle concentration in $\mu g/m^3$ (Table 1).

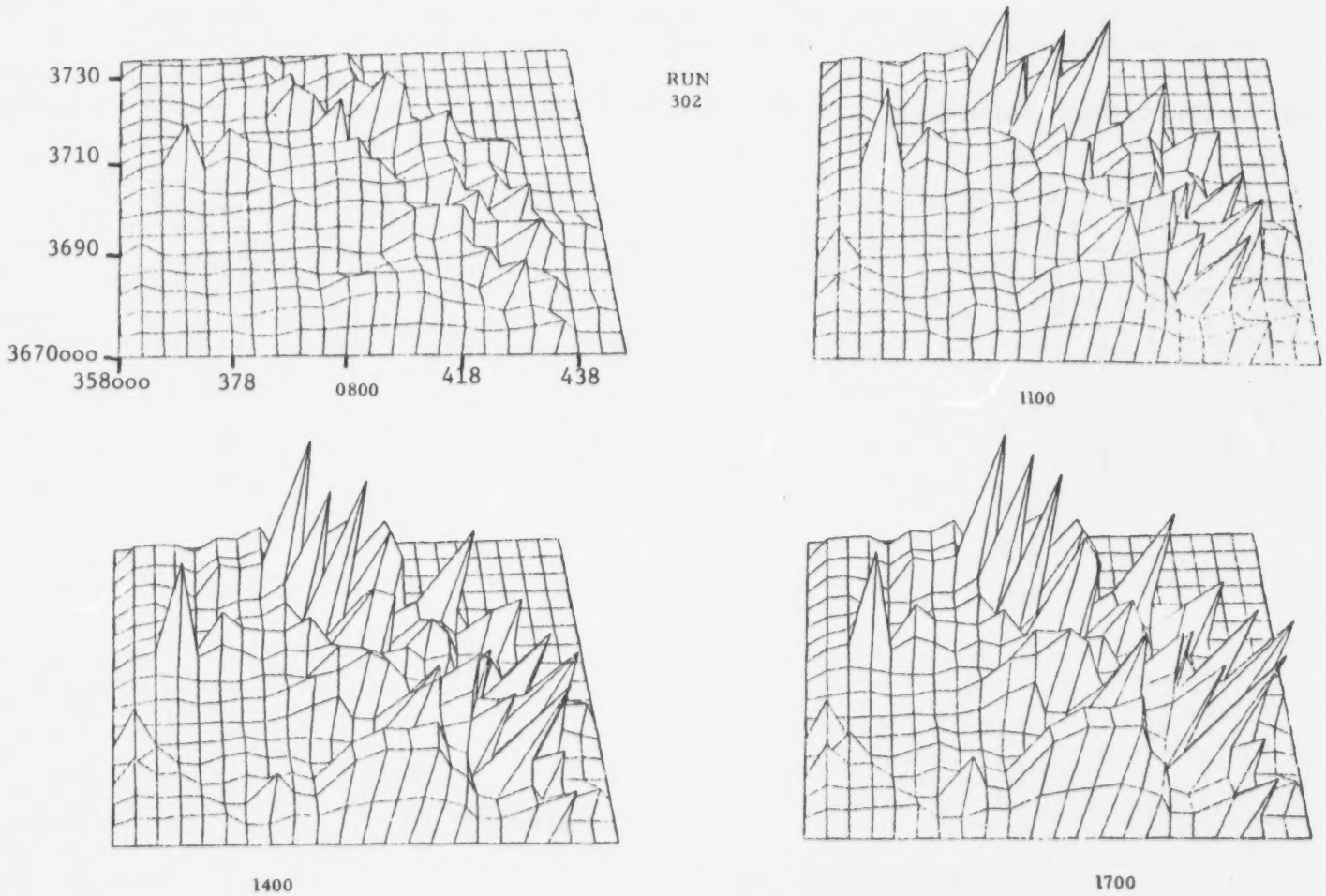

Figure 7. Dust Concentration at 10m for Maricopa County, Arizona, UTM Easting 358ooo to 446ooo, UTM Northing 3670ooo to 3734ooo.

Particle Size: 5 μm, Wind Field: 4X. Gravitational Sedimentation and Deposition not Operating. Height above surface proportional to particle concentration in $\mu g/m^3$.

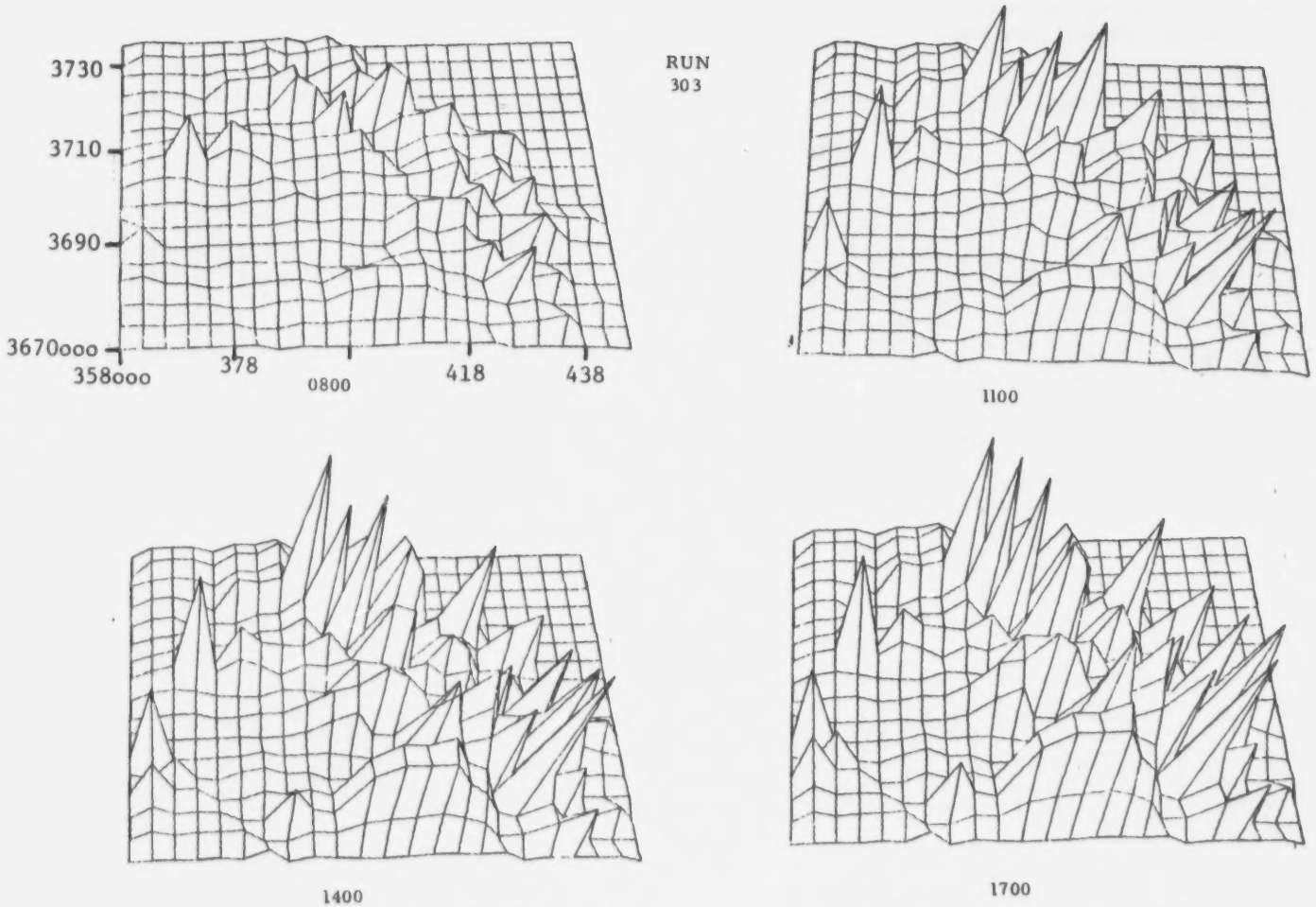

Figure 8. Dust Concentration at 10m for Maricopa County, Arizona, UTM Easting 358ooo to 446ooo, UTM Northing 3670ooo to 3734ooo.

Particle Size: 20 µm, Wind Field: 4X. Gravitational Sedimentation and Deposition not Operating. Height above surface proportional to particle concentration in $\mu g/m^3$.

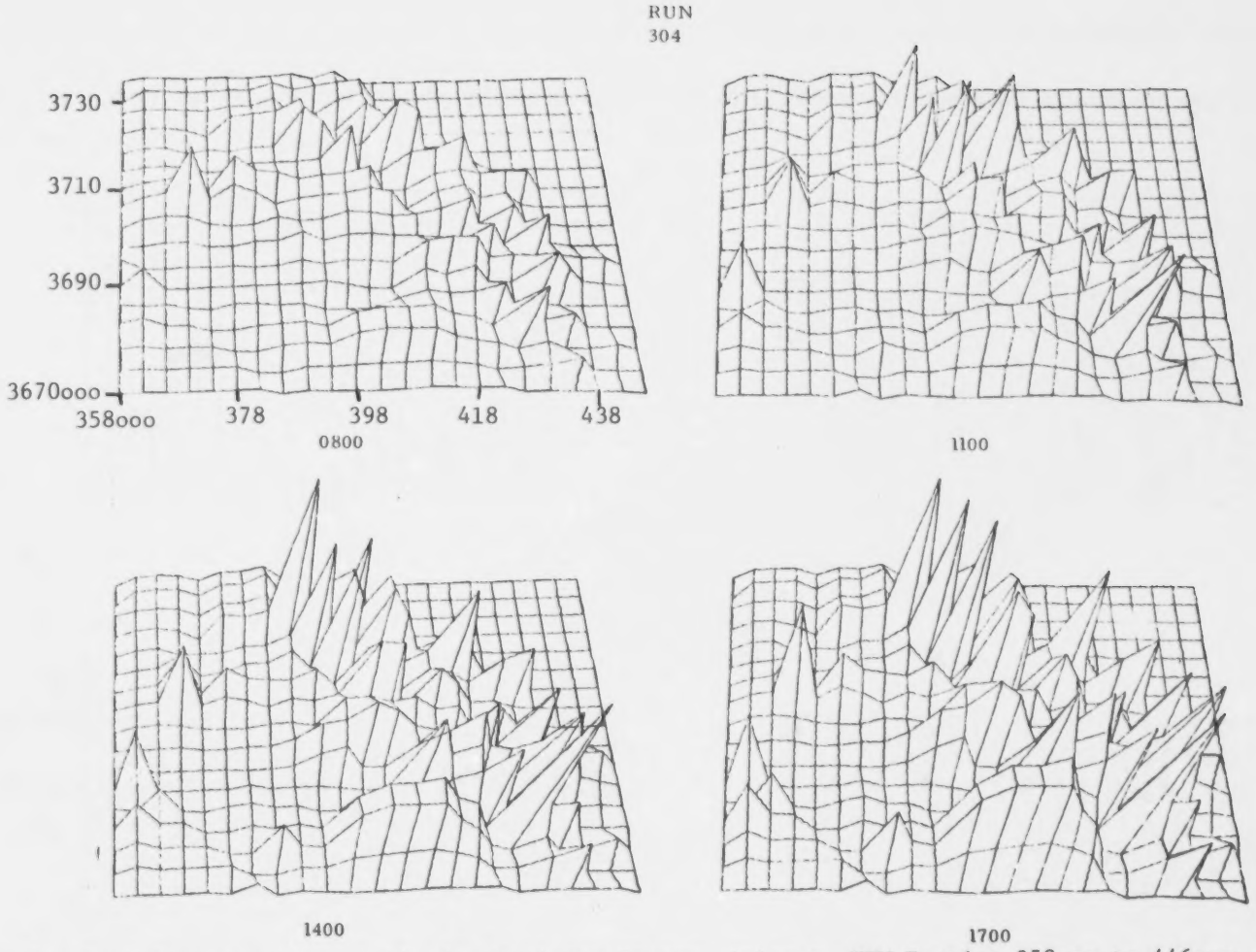

Figure 9. Dust Concentration at 10m for Maricopa County, Arizona, UTM Easting 358ooo to 446ooo, UTM Northing 3670ooo to 3734ooo.

Particle Size: 20 μm, Wind Field: 2X. Gravitational Sedimentation and Deposition not Operating. Height above surface proportional to particle concentration in $\mu g/m^3$.

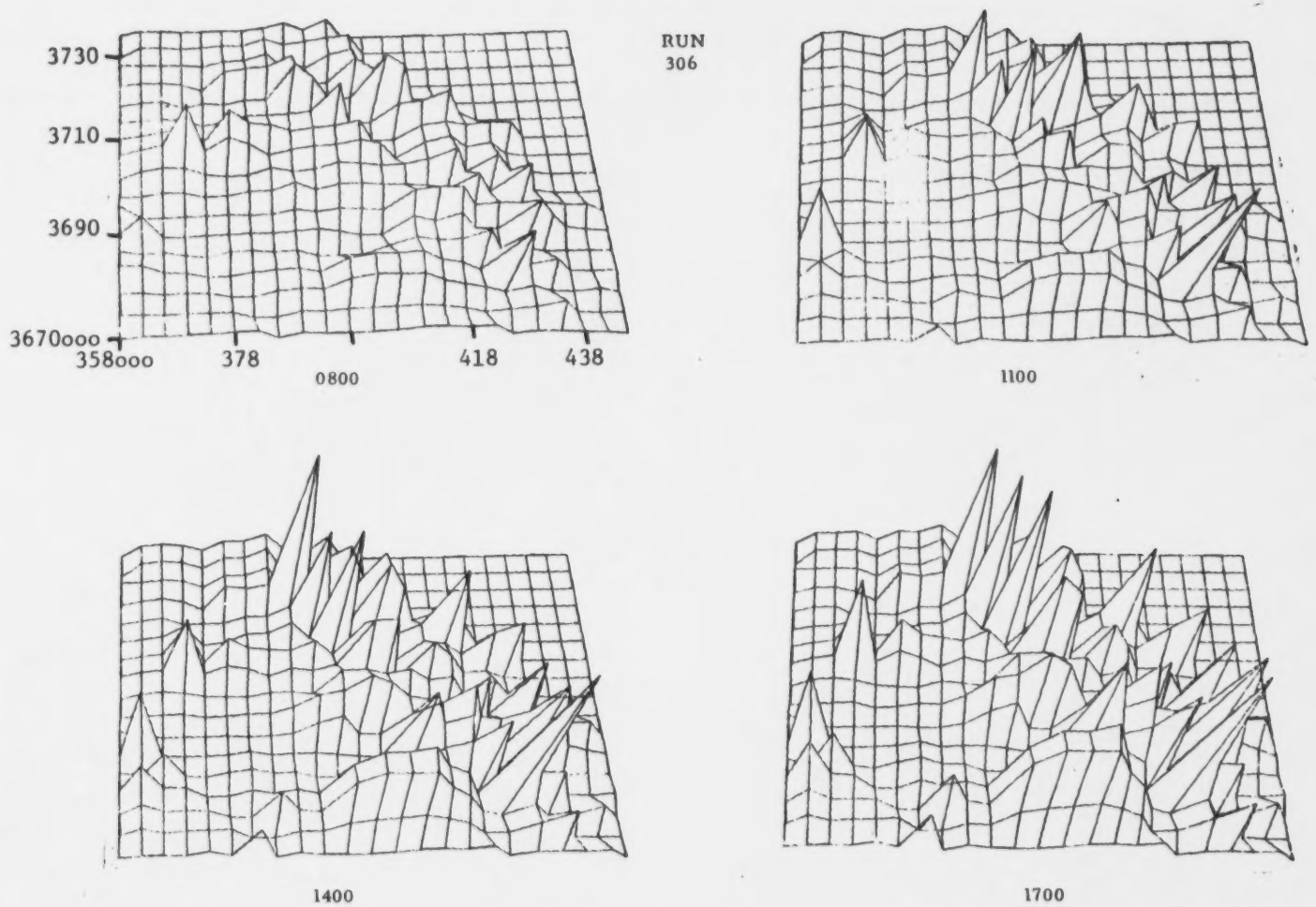

Figure 10. Dust Concentration at 10m for Maricopa County, Arizona, UTM Easting 358ooo to 446ooo, UTM Northing 3670ooo to 3734ooo.

Particle Size: 5 μm, Wind Field: 2X. Gravitational Sedimentation and Deposition Operating. Height above surface proportional to particle concentration in $\mu g/m^3$.

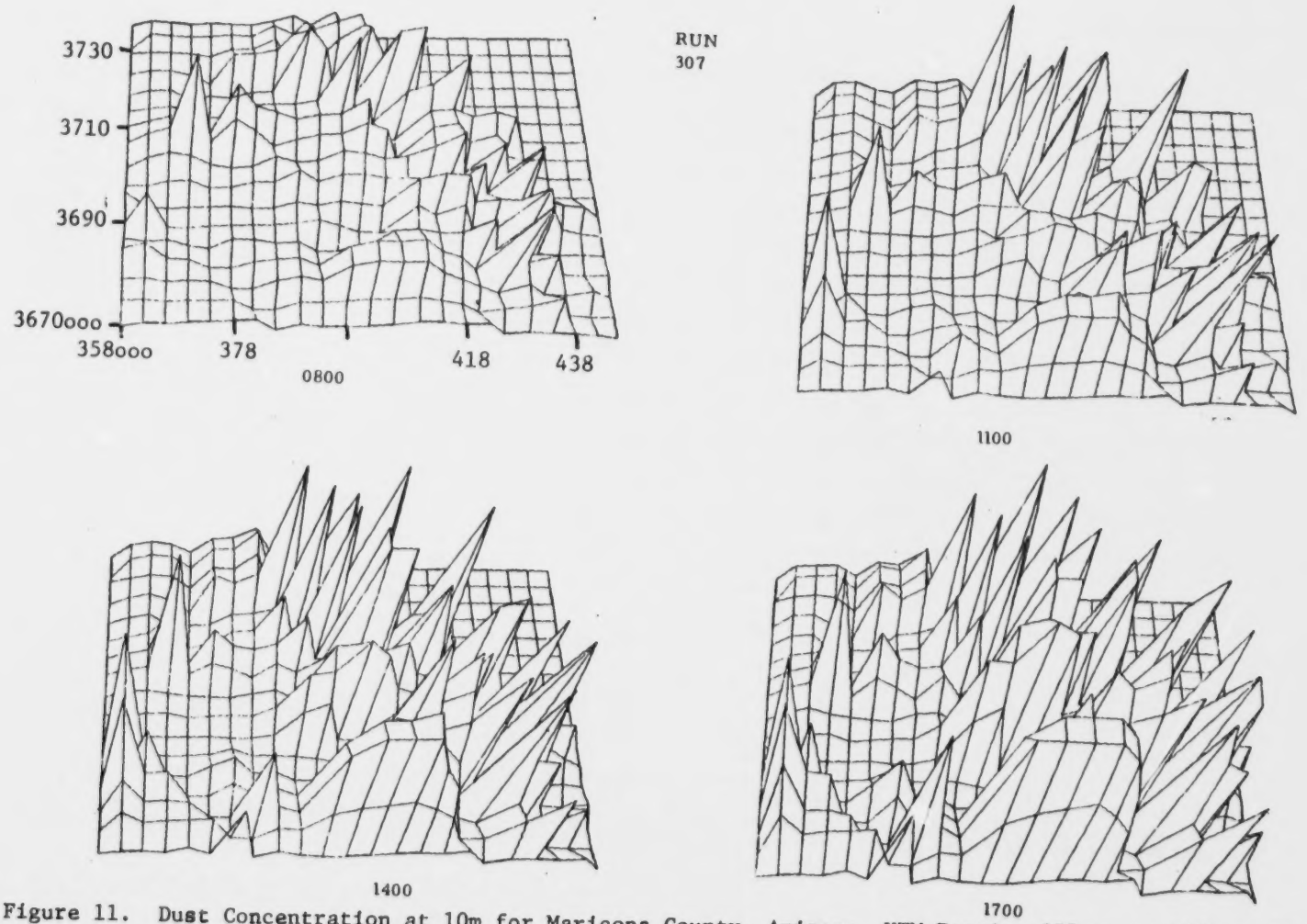

Figure 11. Dust Concentration at 10m for Maricopa County, Arizona, UTM Easting 358ooo to 446ooo, UTM Northing 3670ooo to 3734ooo.

Particle Size: 20 μm, Wind Field: 2X. Gravitational Sedimentation and Deposition Operating. Height above surface proportional to particle concentration in $\mu g/m^3$.

TABLE 1. CALCULATED HOURLY PARTICULATE CONCENTRATIONS ($\mu g/m^3$) AT 10 METERS ABOVE THE SURFACE. (See Fig. 4).

0800 LST

IUTM =		358	362	366	370	374	378	382	386	390	394	398	402	406	410	414	418	422	426	430	434	438	442	446
I =		1	2	3	4	5	6	7	8	9	10	11	12	13	14	15	16	17	18	19	20	21	22	23
3734	17	71	92	85	76	79	76	69	87	116	64	134	1	0	0	0	1	0	1	0	0	2	0	0
3730	16	25	95	87	78	81	86	80	126	87	106	125	136	0	0	0	0	0	0	0	0	0	0	0
3726	15	94	87	86	81	69	97	98	142	29	35	130	159	0	0	0	0	0	0	0	0	0	0	0
3722	14	65	80	78	64	12	148	169	180	242	35	47	222	139	37	0	0	0	0	0	0	0	0	0
3718	13	46	64	68	20	47	28	60	63	317	210	59	64	351	281	35	41	0	0	0	0	0	0	0
3714	12	48	55	67	49	11	24	76	80	87	103	291	0	0	150	166	230	58	0	0	0	0	0	0
3710	11	65	81	110	133	23	273	169	148	99	117	129	163	0	0	119	143	115	128	119	0	0	0	0
3706	10	85	122	156	462	100	215	147	52	93	115	126	157	126	0	132	175	85	115	23	0	0	0	0
3702	9	33	103	132	123	57	41	45	107	69	85	136	125	99	110	145	232	37	178	40	22	0	0	0
3698	8	36	37	73	69	23	29	72	77	144	71	117	118	99	101	87	50	179	24	249	24	0	0	2
3694	7	138	13	11	25	25	33	26	34	78	45	71	66	54	219	244	236	84	99	93	92	69	63	2
3690	6	55	194	7	6	21	28	35	39	52	70	41	0	0	161	118	185	53	43	278	151	42	16	5
3686	5	78	44	57	19	0	56	59	46	54	0	0	0	92	169	139	142	214	47	42	14	10	10	4
3682	4	136	124	49	44	0	0	43	65	80	40	169	207	203	223	149	114	41	377	85	127	14	3	13
3678	3	58	49	35	45	40	0	0	58	92	73	179	218	214	220	146	105	73	19	80	18	13	41	0
3674	2	42	38	33	46	49	56	0	0	61	60	81	95	104	118	102	78	28	54	79	132	15	5	5
3670	1	8	38	36	53	63	77	82	0	63	52	58	66	89	124	124	108	116	28	51	49	40	35	5

UTM Northing

(Continued)

TABLE 1. (Continued)

1100 LST

IUTM =		358	362	366	370	374	378	382	386	390	394	398	402	406	410	414	418	422	426	430	434	438	442	446
I =		1	2	3	4	5	6	7	8	9	10	11	12	13	14	15	16	17	18	19	20	21	22	23
3734	17	32	97	102	73	58	112	107	122	61	39	102	3	0	0	0	0	0	0	0	0	1	0	0
3730	16	11	94	102	71	51	120	114	138	31	42	81	140	0	0	0	0	0	0	0	0	0	0	0
3726	15	83	85	99	69	40	122	119	142	14	14	71	118	2	1	0	0	0	0	0	0	0	0	0
3722	14	47	74	90	52	11	155	136	153	516	17	19	121	256	58	0	0	0	0	0	1	0	0	0
3718	13	39	61	80	33	32	41	84	89	134	338	25	26	449	209	30	62	0	0	0	0	0	0	0
3714	12	32	51	73	143	8	31	85	90	95	41	486	0	0	45	101	292	150	0	0	0	0	0	0
3710	11	33	53	78	247	19	163	104	90	105	123	48	220	0	0	90	137	38	164	179	0	0	0	0
3706	10	35	59	81	342	55	99	77	43	85	84	92	222	261	0	160	150	41	64	10	1	0	0	0
3702	9	14	44	59	47	33	29	28	56	67	35	150	144	121	143	123	132	17	97	21	9	0	0	0
3698	8	16	18	31	37	15	21	34	33	80	112	139	189	172	141	103	35	211	14	276	12	0	0	1
3694	7	62	16	5	9	12	18	11	14	34	80	117	42	20	160	213	265	106	99	120	99	72	71	4
3690	6	24	425	8	3	9	17	37	19	23	32	13	0	0	325	163	218	26	21	353	184	51	24	5
3686	5	35	17	112	8	0	38	54	22	44	0	0	0	86	56	160	182	295	27	21	7	4	12	4
3682	4	51	194	51	58	0	0	41	69	64	25	195	250	248	271	176	137	24	685	119	143	7	2	13
3678	3	21	81	35	43	40	0	0	112	68	44	210	259	257	262	177	126	44	12	83	9	6	60	0
3674	2	14	60	33	44	48	55	0	0	59	58	97	114	125	142	123	96	43	46	97	164	8	2	3
3670	1	4	22	26	36	57	28	179	3	62	44	41	49	62	83	93	92	116	40	68	70	66	69	10

UTM Northing

(Continued)

TABLE 1. (Continued)

1400 LST

IUTM =	358	362	366	370	374	378	382	386	390	394	398	402	406	410	414	418	422	426	430	434	438	442	446
I =	1	2	3	4	5	6	7	8	9	10	11	12	13	14	15	16	17	18	19	20	21	22	23
3734	17	32	94	106	97	63	117	120	151	60	36	121	4	0	0	0	0	0	0	0	0	1	0	0
3730	16	11	87	99	94	56	115	115	160	31	41	103	168	0	0	0	0	0	0	0	0	0	0	0
3726	15	75	77	91	88	43	112	111	151	15	14	86	95	3	1	0	0	0	0	0	0	0	0	0
3722	14	42	68	81	64	12	143	124	152	850	18	19	119	319	56	1	1	0	0	0	0	0	0	0
3718	13	35	57	71	37	33	38	73	74	103	556	26	26	312	197	37	102	0	0	0	0	0	0	0
3714	12	30	48	65	156	7	28	75	80	146	39	623	0	0	45	116	407	147	0	0	0	0	0	0
3710	11	32	53	72	257	18	155	98	83	85	139	45	250	0	0	134	108	37	177	233	0	0	0	0
3706	10	35	61	77	346	54	99	74	39	87	61	104	391	398	0	249	153	41	47	10	1	0	0	0
3702	9	14	47	58	46	31	28	27	53	61	33	197	205	182	203	128	128	17	111	22	9	0	0	0
3698	8	16	19	31	35	14	21	34	[illegible]	79	176	196	296	252	158	127	50	265	15	346	13	0	0	1
3694	7	57	21	5	10	12	18	11	14	34	116	160	25	18	157	229	334	151	127	185	136	96	92	5
3690	6	24	482	9	3	9	17	47	18	24	25	13	0	0	456	249	289	28	22	459	243	76	39	7
3686	5	34	18	197	8	0	38	68	31	38	0	0	0	135	56	221	261	406	30	23	8	5	18	4
3682	4	47	260	78	80	0	0	53	27	55	26	250	332	336	362	244	188	27	850	199	189	7	2	18
3678	3	20	113	50	59	56	0	0	217	64	45	280	351	353	356	248	173	48	14	109	10	6	90	0
3674	2	14	82	46	58	65	73	0	0	56	59	135	163	178	199	172	135	58	47	132	218	8	3	3
3670	1	3	19	27	27	64	23	265	11	62	45	41	49	63	83	93	92	115	40	71	77	74	87	14

UTM Northing

(Continued)

TABLE 1. (Continued)

1700 LST

IUTM =		358	362	366	370	374	378	382	386	390	394	398	402	406	410	414	418	422	426	430	434	438	442	446
I =		1	2	3	4	5	6	7	8	9	10	11	12	13	14	15	16	17	18	19	20	21	22	23
3734	17	62	129	134	135	92	144	139	183	106	59	190	2	0	0	0	1	0	1	0	0	2	0	0
3730	16	23	126	130	131	88	150	141	207	64	82	154	221	0	0	0	0	0	0	0	0	0	0	0
3726	15	110	114	124	120	71	156	147	205	27	31	125	143	1	0	0	2	0	0	0	0	0	0	0
3722	14	67	104	110	79	14	218	194	219	850	33	41	213	366	51	1	1	0	0	0	0	0	0	0
3718	13	52	87	95	27	49	40	99	100	204	831	53	55	472	313	47	89	0	0	0	0	0	0	0
3714	12	47	74	87	107	11	28	106	113	191	77	850	0	0	99	199	584	112	0	0	0	0	0	0
3710	11	58	90	118	270	25	282	172	146	123	195	91	276	0	0	223	151	83	238	332	0	0	0	0
3706	10	74	118	147	686	99	201	138	62	138	108	171	628	540	0	364	244	74	83	21	0	0	0	0
3702	9	33	98	123	103	61	49	47	103	88	70	304	317	277	280	160	220	35	178	38	20	0	0	0
3698	8	36	39	72	73	24	34	69	72	147	268	298	436	366	189	187	71	386	25	504	23	0	0	2
3694	7	130	17	13	23	25	36	26	35	74	165	234	45	35	237	335	498	222	192	269	203	142	141	6
3690	6	55	602	9	6	20	33	75	34	46	55	27	0	0	661	372	434	52	42	680	361	111	60	12
3686	5	78	32	290	17	0	65	111	60	63	0	0	0	222	111	339	386	602	48	42	14	10	27	8
3682	4	105	393	126	116	0	0	83	47	92	40	374	497	503	548	367	282	43	850	291	277	14	3	30
3678	3	44	168	82	94	89	0	0	311	106	72	426	531	534	538	375	261	74	20	164	18	12	137	0
3674	2	30	121	74	93	103	116	0	0	83	83	205	249	272	301	261	203	49	68	195	319	15	5	5
3670	1	11	36	44	51	92	50	352	20	88	68	68	79	104	138	145	134	161	38	84	94	89	103	17

UTM Northing

TABLE 2. CALCULATED HOURLY PARTICULATE CONCENTRATIONS ($\mu g/m^3$) AT 10 METERS ABOVE THE SURFACE. (See Fig. 6)

0800 LST

IUTM =	358	362	366	370	374	378	382	386	390	394	398	402	406	410	414	418	422	426	430	434	438	442	446
1 =	1	2	3	4	5	6	7	8	9	10	11	12	13	14	15	16	17	18	19	20	21	22	23
3734	17	73	93	85	75	80	76	69	87	119	65	136	1	0	0	0	1	0	1	0	0	2	0	0
3730	16	25	111	103	92	97	103	95	152	107	132	159	175	0	0	0	0	0	0	0	0	0	0	0
3726	15	96	102	102	96	80	120	122	174	30	36	163	207	0	0	0	0	0	0	0	0	0	0	0
3722	14	67	94	91	72	12	189	200	215	316	38	48	286	172	38	0	0	0	0	0	0	0	0	0
3718	13	47	74	80	20	49	31	70	75	387	290	61	69	404	368	35	42	0	0	0	0	0	0	0
3714	12	49	66	80	49	11	24	96	103	106	132	409	0	0	185	210	307	65	0	0	0	0	0	0
3710	11	67	100	136	144	24	335	208	182	123	152	165	219	0	0	152	178	141	159	146	0	0	0	0
3706	10	87	147	180	609	103	255	180	67	118	147	157	208	171	0	171	215	107	147	23	0	0	0	0
3702	9	34	117	157	136	68	45	57	135	90	105	172	157	125	140	193	279	38	223	43	22	0	0	0
3698	8	36	38	81	83	29	37	88	90	178	90	146	144	123	125	104	60	228	25	315	24	0	0	2
3694	7	141	14	12	27	30	39	28	36	92	56	88	79	65	264	298	288	103	122	114	114	84	75	2
3690	6	56	249	7	7	24	33	42	47	64	86	50	0	0	196	141	219	54	43	335	178	51	19	5
3686	5	80	55	69	19	0	68	74	57	67	0	0	0	119	199	166	173	266	48	43	14	10	12	4
3682	4	142	163	61	56	0	0	53	81	97	46	200	244	240	263	179	139	42	481	103	162	14	3	13
3678	3	60	64	43	55	49	0	0	73	113	89	214	259	255	261	174	125	77	19	98	18	13	51	0
3674	2	43	49	42	58	60	69	0	0	74	73	97	114	125	142	122	93	29	60	93	161	15	5	5
3670	1	8	40	37	55	65	80	85	0	64	52	59	68	91	127	128	111	119	28	52	50	41	36	5

UTM Northing

(Continued)

TABLE 2. (Continued)

1100 LST

IUTM =		358	362	366	370	374	378	382	386	390	394	398	402	406	410	414	418	422	426	430	434	438	442	446
I =		1	2	3	4	5	6	7	8	9	10	11	12	13	14	15	16	17	18	19	20	21	22	23
3734	17	33	102	105	74	59	117	111	125	62	40	102	3	0	0	0	0	0	0	0	0	1	0	0
3730	16	11	112	121	81	59	150	140	170	35	49	100	187	0	0	0	0	0	0	0	0	0	0	0
3726	15	85	101	118	77	44	153	147	172	14	14	81	164	3	1	0	0	0	0	0	0	0	0	0
3722	14	47	90	109	56	12	196	163	185	642	17	19	155	346	69	1	0	0	0	0	2	0	0	0
3718	13	39	74	99	34	34	49	109	120	165	454	26	27	535	285	32	70	0	0	0	0	0	0	0
3714	12	33	61	90	165	8	35	111	118	119	46	759	0	0	44	125	409	170	0	0	0	0	0	0
3710	11	34	62	95	310	21	195	124	106	139	167	59	479	0	0	119	185	42	220	222	0	0	0	0
3706	10	36	66	91	456	59	108	88	54	114	110	110	361	486	0	215	188	48	83	10	1	0	0	0
3702	9	15	47	65	47	40	35	34	64	90	38	191	183	158	192	166	156	17	112	22	9	0	0	0
3698	8	16	18	33	43	17	26	38	36	94	144	175	238	222	183	128	41	266	14	342	12	0	0	1
3694	7	62	17	5	9	14	19	11	15	36	101	148	50	22	189	260	329	132	121	147	122	89	87	4
3690	6	24	538	8	3	10	19	45	21	25	37	13	0	0	410	198	264	27	21	431	222	63	29	5
3686	5	35	17	138	8	0	50	74	27	56	0	0	0	121	56	196	226	366	27	21	8	4	15	4
3682	4	50	281	67	91	0	0	53	92	79	27	236	302	299	327	215	170	25	850	145	180	7	2	13
3678	3	21	113	45	56	50	0	0	143	88	50	255	315	313	318	215	153	46	13	102	10	6	74	0
3674	2	14	82	43	57	61	69	0	0	74	72	118	139	153	173	150	117	46	52	118	201	8	3	3
3670	1	4	23	27	38	58	28	186	4	64	47	42	49	63	83	94	93	118	40	69	72	67	71	11

UTM Northing

(Continued)

TABLE 2. (Continued)

1400 LST

IUTM =	358	362	366	370	374	378	382	386	390	394	398	402	406	410	414	418	422	426	430	434	438	442	446
I =	1	2	3	4	5	6	7	8	9	10	11	12	13	14	15	16	17	18	19	20	21	22	23
3734	17	32	96	108	97	63	121	126	158	60	36	118	3	0	0	0	0	0	0	0	1	0	0
3730	16	11	100	114	107	64	139	140	199	34	47	125	243	0	0	0	0	0	0	0	0	0	0
3726	15	76	87	105	99	47	135	135	185	16	14	99	131	5	2	0	0	0	0	0	0	0	0
3722	14	43	77	93	68	13	173	143	180	850	19	19	145	457	67	1	0	0	0	1	0	0	0
3718	13	35	65	83	38	34	42	88	93	104	774	27	27	362	270	39	125	0	0	0	0	0	0
3714	12	30	56	76	180	8	30	92	100	207	41	850	0	0	44	145	635	158	0	0	0	0	0
3710	11	32	61	85	328	19	180	144	95	113	197	47	547	0	0	192	130	39	242	294	0	0	0
3706	10	35	68	87	472	56	109	83	47	112	74	130	679	726	0	360	189	47	50	11	0	0	0
3702	9	15	50	64	47	36	33	32	61	78	34	258	270	248	284	177	147	17	131	23	9	0	0
3698	8	16	19	33	41	17	25	37	35	91	233	251	381	331	202	156	60	335	15	428	13	0	0
3694	7	57	21	5	10	13	20	11	14	36	150	203	25	18	177	277	417	193	157	229	168	118	113
3690	6	24	607	9	3	10	19	58	22	27	26	13	0	0	574	304	350	29	22	558	294	93	48
3686	5	34	19	244	8	0	50	95	33	45	0	0	0	206	57	273	325	505	31	23	8	5	22
3682	4	48	388	167	123	0	0	70	34	65	28	303	402	404	436	301	235	29	850	243	238	7	2
3678	3	20	166	68	79	72	0	0	298	81	51	344	429	431	434	303	211	51	15	133	11	6	112
3674	2	14	112	63	78	85	95	0	0	70	71	168	202	221	245	212	166	60	52	160	266	8	3
3670	1	4	19	28	28	66	24	277	11	64	46	42	49	64	84	95	94	117	41	72	78	75	89

UTM Northing

(Continued)

TABLE 2. (Continued)

1700 LST

IUTM =		358	362	366	370	374	378	382	386	390	394	398	402	406	410	414	418	422	426	430	434	438	442	446
I =		1	2	3	4	5	6	7	8	9	10	11	12	13	14	15	16	17	18	19	20	21	22	23
3734	17	63	131	135	133	93	146	141	187	109	60	187	2	0	0	0	1	0	1	0	0	2	0	0
3730	16	24	158	167	167	110	208	195	289	75	100	224	396	0	0	0	0	0	0	0	0	0	0	0
3726	15	112	142	159	149	83	219	205	283	28	31	163	208	3	1	0	0	0	0	0	0	0	0	0
3722	14	68	132	141	83	14	311	245	288	850	35	42	296	663	63	1	0	0	0	0	1	0	0	0
3718	13	53	111	126	27	52	47	138	148	211	850	55	59	565	500	50	120	0	0	0	0	0	0	0
3714	12	48	99	119	123	12	30	154	166	326	83	850	0	0	100	295	850	138	0	0	0	0	0	0
3710	11	60	117	157	366	26	365	222	184	175	330	97	700	0	0	420	167	96	389	493	0	0	0	0
3706	10	76	142	179	850	103	237	170	88	212	134	247	850	850	0	689	360	93	104	22	0	0	0	0
3702	9	33	108	144	105	80	64	63	131	133	73	484	514	468	482	246	272	35	234	40	21	0	0	0
3698	8	37	40	79	92	33	48	83	83	188	48	456	668	581	274	259	96	566	25	713	23	0	0	2
3694	7	133	17	13	24	30	42	27	36	84	263	348	46	36	293	451	706	332	273	387	288	199	195	5
3690	6	56	850	9	7	23	41	110	39	56	59	28	0	0	850	523	590	53	43	850	481	154	85	13
3686	5	80	34	417	18	0	97	200	85	88	0	0	0	470	113	487	552	850	49	42	14	10	38	8
3682	4	109	790	221	221	0	0	136	52	122	45	509	671	676	735	527	405	44	850	410	401	14	4	30
3678	3	45	315	142	158	141	0	0	562	150	90	596	736	742	746	525	364	79	21	220	18	13	195	0
3674	2	31	213	130	156	166	183	0	0	116	114	297	363	396	431	371	287	50	79	268	436	15	5	5
3670	1	11	37	46	53	95	51	373	21	91	70	68	80	105	140	148	137	165	39	86	97	92	106	18

UTM Northing

A number of parameters were varied in the model study. Two mean particle sizes were used for the suspended particles: 5 μm equivalent diameter and 20 μm equivalent diameter. Wind speeds were varied as 1x, 2x, and 4x the wind vector components of Berman and DeLaney (10). The model runs presented cover the time 0600 - 1900 LST during which constant daytime wind fields (10) were used. Obviously this procedure is not correct, but suitable for the purposes of our model studies. Finally, identical runs were carried out with gravitational sedimentation and dry deposition "switched off" and "switched on" according to current estimates (14).

Figs. 4 to 11 give these model studies for the hourly average particle concentrations at 10 m. from 0800 to 1700 LST. Tables 1 and 2 give a quantitative assessment of particle concentration values indicated in the Fig. 4 and Fig. 6. The height above the baseline surface in these figures is proportional to the particle concentration. In the figures, the maximum particle concentration shown is 850 $\mu g/m^3$.

In considering the information presented in the figures, the very complex topography and wind fields in Maricopa County must be kept in mind (see Figs. 1 to 2). Some of the results are not intuitively obvious and arise from the complex dynamical relationships between source strength variation in space and time, advection, vertical dispersion, sedimentation, and dry deposition.

Several features are common to all model runs. Outstanding is the somewhat localized nature of particle concentration maxima. Maxima tend to remain centered over their initial positions during the course of the day. This behavior is attributed to the relatively low wind speeds studied and to the relatively rapid vertical transport and deposition processes.

In some cases, near the base of North Mountain for example, there is evidence of advective transport and accumulation of dust. However, on the whole, large amounts of dust do not appear to be advected for distances greater than a few grid squares (4 km. x 4 km.). Another feature is the monotonic growth of most of the maxima during the course of the day. However, some of the maxima tend to decrease after 1000 or 1100 LST and to increase again after 1500 or 1600 LST owing to the particular nature of the sources

at these locations. For a pollutant such as CO, which is almost entirely derived from automotive emissions, the hourly variation of traffic density combines with the increase in mixing height during the first part of the day to give a variation of CO concentration with time. This variation consists of two maxima and a minimum in the mid-afternoon (10). For dust, over 60% of the estimated emissions are not related to traffic, there is not a pronounced mid-afternoon mimimum in dust emissions. Also, our emissions data are averaged over a 4 km. x 4 km. grid and do not reflect specific roadside concentration levels. The minimum mixing height assumed is 130 m. so that there is not a dramatic change in dust concentration at 10 m. as the mixing height increases during the first part of the day. As will be apparent later, however, such dramatic changes do occur in the dust concentration at greater heights above the surface.

The results of these computer runs are in qualitative agreement with available data (9). For example, it was observed (9) that the average surface (10 m.) particulate mass concentrations at Chandler during the late November 1975 IITRI field study were approximately twice those found in Phoenix. In addition, the average experimental values for mass concentration reported (9) for Phoenix (203 $\mu g/m^3$) and Chandler (431 $\mu g/m^3$) are in approximate comparison with the calculated results of runs 298 and 300, given in Tables 1 and 2. Owing to insufficient data, we have carried out model studies and did not attempt to simulate exactly the complex meteorological conditions that occurred during the IITRI study.

EFFECT ON 10 m. DUST CONCENTRATION OF VARIATION IN MEAN PARTICLE SIZE

Comparison may be made between runs 298 and 300. Run 298 assumes mean suspended particle diameter of 5 μm, the wind field (1x) of Berman and DeLaney (10), and the presence of gravitational sedimentation and dry deposition (14). Run 300 only differs from 298 in the assumption of mean suspended particle diameter of 20 μm. Examination of Figs. 4 and 6 shows that dust concentrations during the day at 10 m. are higher for the 20 μm mean diameter than for 5 μm. This difference is greater over populated areas (such as Phoenix) where the macro-scale surface roughness is high, with a resultant increase in vertical transport rates. These increased rates tend to magnify the effects of the different sedimentation rates on

the 10 m. dust concentrations for 5 μm and 20 μm particles. Outside the built-up areas, the 10 m. dust concentrations for 20 μm mean diameter particles (run 300) are only slightly greater than those for 5 μm (run 298).

EFFECT ON 10 m. DUST CONCENTRATION OF VARIATION IN WIND SPEED

Wind speed is varied for fixed particle size (5 μm) with deposition and gravitational sedimentation shown in Figures 4 and 10 (runs 298 and 306). The latter run is for a wind field exactly twice that of the former. The increased wind field means that the friction velocity is increased, which has the effect of increasing the vertical dispersion rate. Intercomparison of hourly values for runs 298 and 306 shows that the concentration levels for run 298 are usually somewhat larger than for run 306. The increased vertical dispersion and deposition rates for run 306 lowers the 10 m. dust concentrations relative to those for run 298. An analogous comparison is afforded by the results of Figures 6 and 11 (runs 300 and 307) for 20 μm mean particle size. 10 m. particle concentrations are much greater for run 307 which has twice the wind speed of run 300. The explanation for the larger concentrations is related to the complex interrelationships of source strength, surface roughness, advective wind field, and gravitational sedimentation.

This result is opposite to that found for runs 298 and 306 for 5 μm particles. The difference arises in that for the 5 μm particles, gravitational sedimentation is of minor importance. For 20 μm particles, gravitational sedimentation is critical and its interaction with the other processes produces the differences found between runs 300 and 307.

EFFECT ON 10 m. DUST CONCENTRATION OF DEPOSITION AND GRAVITATIONAL SEDIMENTATION

These effects are closely related to particle size. Consider runs 298 and 299 for 5 μm particles with and without deposition and gravitational sedimentation. Relative to advective and vertical transfer rates, gravitational sedimentation is negligible for 5 μm particles. Hence, only deposition at the surface is of importance. Therefore, the 10 m. dust concentrations for run 298, where deposition and sedimentation occur, are slightly lower than those for run 299 where these processes are absent. For 20 μm particles,

gravitational sedimentation is a very important process and the analogous comparison for 20 μm particles is quite different.

Runs 307 and 304 for 20 μm particles compare 10 m. dust concentrations with and without deposition and gravitational sedimentation. In this case the inclusion of gravitational sedimentation results in much higher 10 m. dust concentrations (run 307) than found neglecting this process (run 304).

A study of the variation of the dust concentration with height provides considerable insight into the dynamics of dust transport. Figs. 12 to 17 give dust concentration isopleths in $\mu g/m^3$ in a plane perpendicular to the surface extending in an easterly direction from Tolleson to just east of Scottsdale (see map, Fig. 1). The heights indicated in these figures refer to height above the surface. In this plane, the surface rises to the east from 305 m. (1000 ft.) above sea level at Tolleson to 366 m. (1200 ft.) above sea level at Scottsdale. This particular plane was chosen to correspond to the IITRI study regions. The plane includes Phoenix and Scottsdale and avoids the mountainous terrain which would be encountered by a plane running north-south and including Phoenix. One example of a north-south plane is included (Fig. 17). Its interpretation is difficult because of the mountains immediately north and south of Phoenix.

Discussion will be centered here on Figs. 11 to 16 where the effects of various parameters on the vertical dust concentration profile are studied. The complex surface wind patterns must be noted, Fig. 1. During the day, the general trend in this region is flow from west to east.

Figs. 11 to 16 show a pronounced minimum in dust concentration with height at a UTM Easting of around 394_{000}. Several factors produce this behavior. First, the area source emission strength in this region is almost one-half that of the areas immediately east and west. Second, based on Berman and DeLaney's wind field data (10), the advective flow into this region is so small that the neighboring stronger dust sources have no effect on the dust concentration at 394_{000}. Finally, the roughness, z_o, is small for this region in comparison with, for example, z_o for Phoenix ($> 396_{000}$); this leads to small rates of vertical transport.

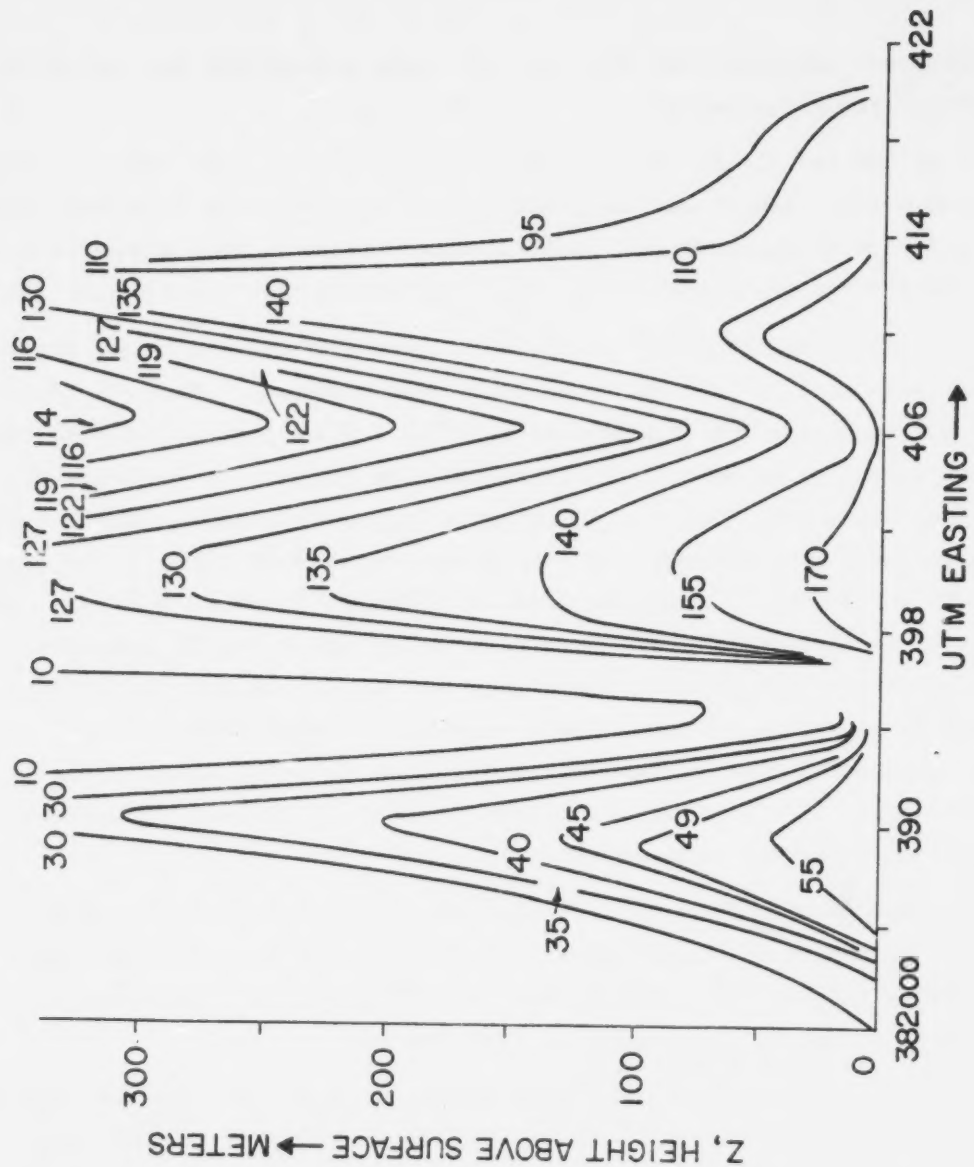

Figure 12. Particle concentration isopleths in $\mu g/m^3$ in plane perpendicular to surface at UTM Northing 3702ooo extending from UTM Easting 382ooo to 422ooo.

Particle Size: 5 μm, Wind Field: 1X. Gravitational sedimentation and deposition operating. Time: 1100 LST.

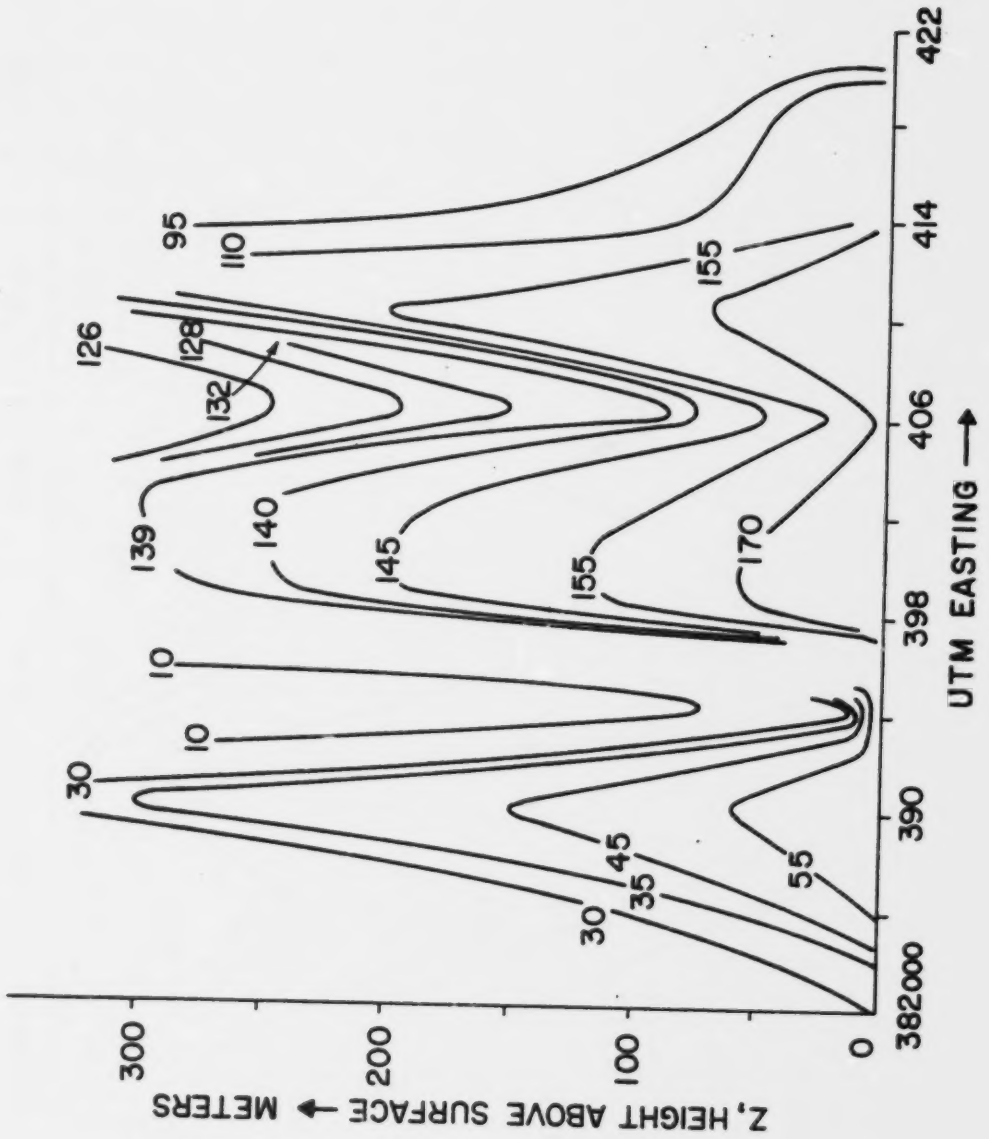

Figure 13. Particle concentration isopleths in $\mu g/m^3$ in plane perpendicular to surface at UTM Northing 3702ooo extending from UTM Easting 382ooo to 422ooo.

Particle Size: 5 μm, Wind Field: 1X. Gravitational sedimentation and deposition not operating. Time: 1100 LST.

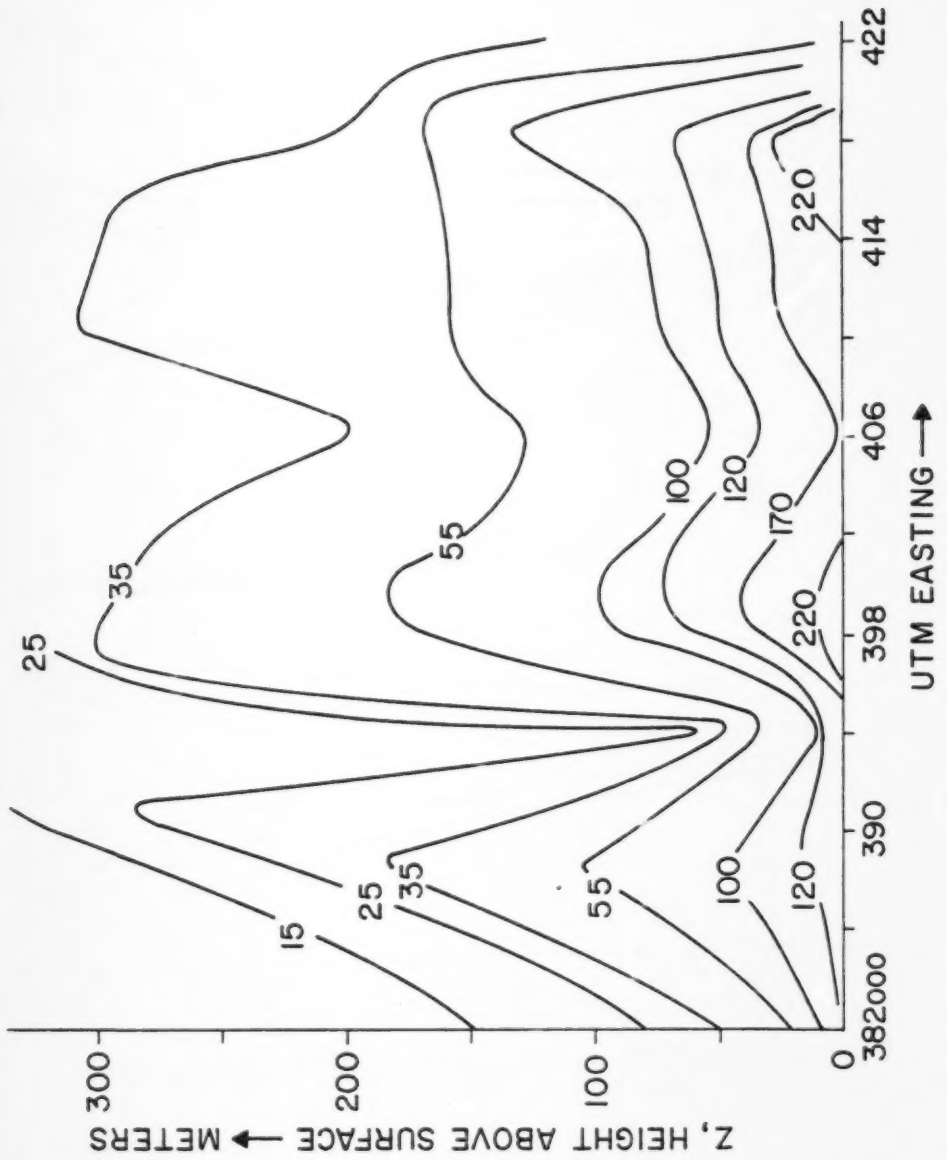

Figure 14. Particle concentration isopleths in $\mu g/m^3$ in plane perpendicular to surface at UTM Northing 3702ooo extending from UTM Easting 382ooo to 422ooo.

Particle Size: 20 μm, Wind Field: 1X. Gravitational sedimentation and deposition operating. Time: 0800 LST.

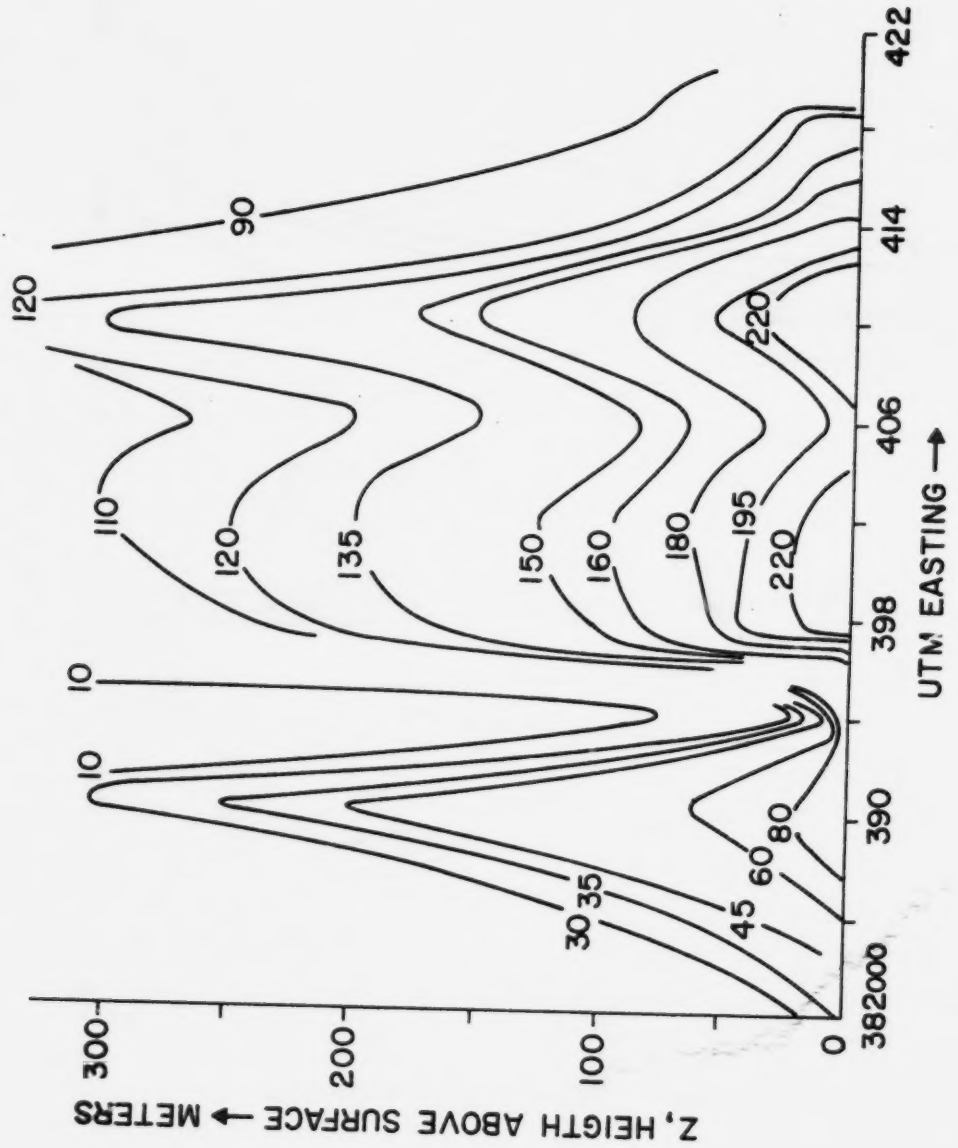

Figure 15. Particle concentration isopleths in $\mu g/m^3$ in plane perpendicular to surface at UTM Northing 3702ooo extending from UTM Easting 382ooo to 422ooo.

Particle Size: 20 μm, Wind Field: 1X. Gravitational sedimentation and deposition operating. Time: 1100 LST.

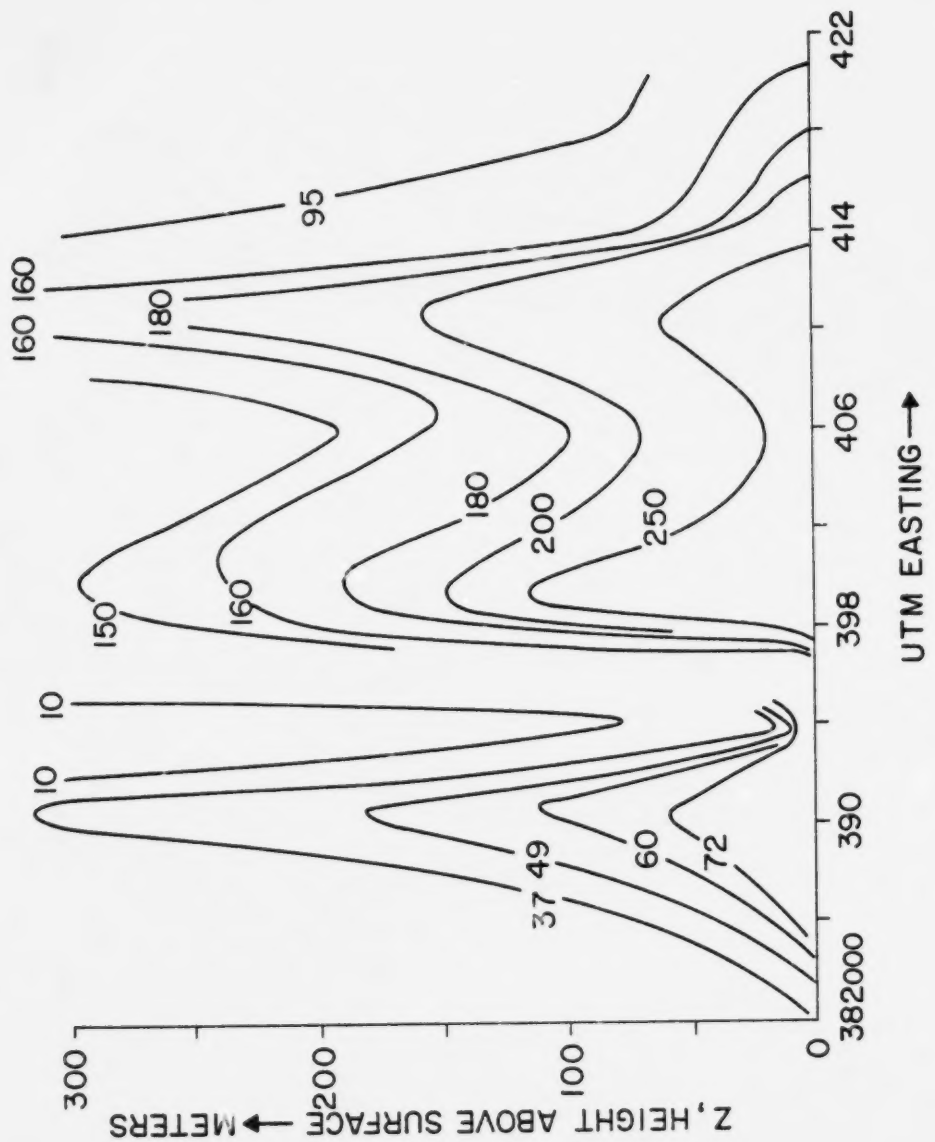

Figure 16. Particle concentration isopleths in $\mu g/m^3$ in plane perpendicular to surface at UTM Northing 3702ooo extending from UTM Easting 382ooo to 422ooo.

Particle Size: 20 μm, Wind Field: 2X. Gravitational sedimentation and deposition operating. Time: 1100 LST.

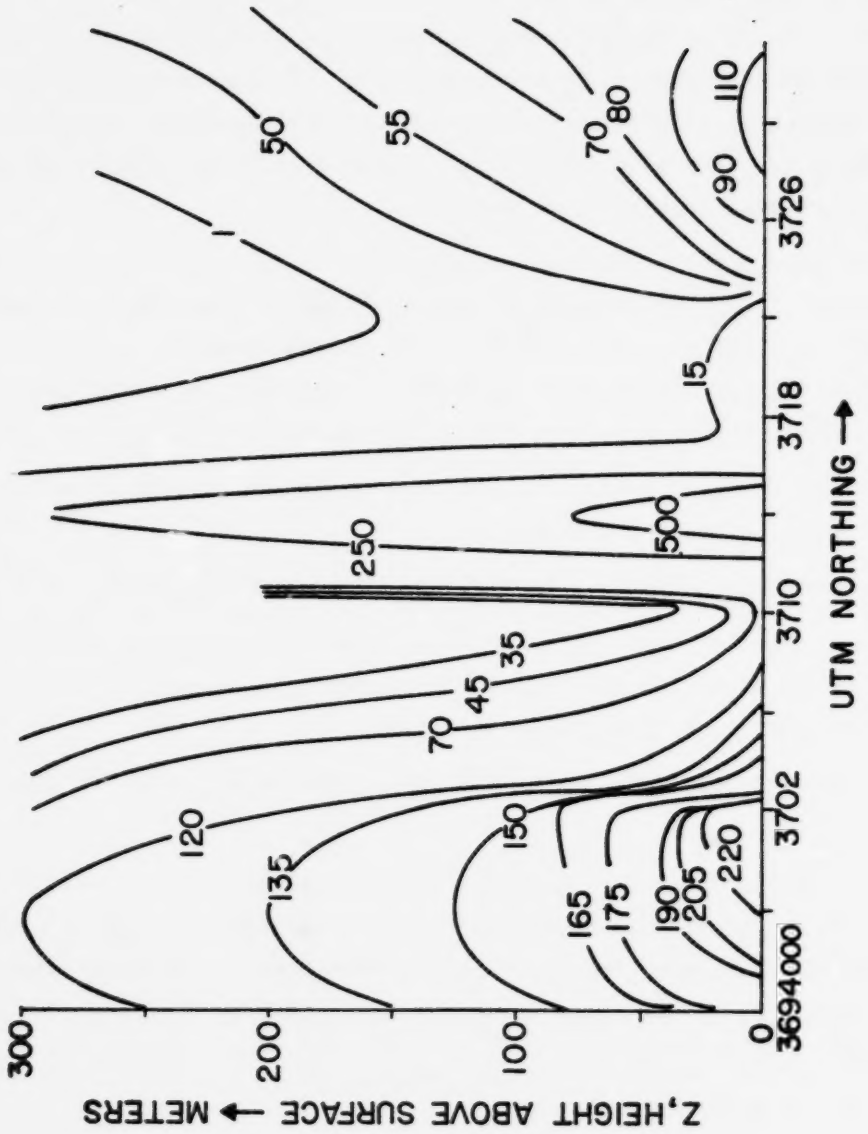

Figure 17. Particle concentration isopleths in $\mu g/m^3$ in plane perpendicular to surface at UTM Easting 398000 extending from UTM Northing 3694000 to 3734000.

Particle Size: 20 μm, Wind Field: 1X. Gravitational sedimentation and deposition operating. Time: 1100 LST.

Figs. 11 to 16 show a rapid rise in dust concentration with height once the area of Phoenix is entered (UTM Easting 396_{000} - 402_{000}). This is due to greatly increased source strengths in the city proper and also to larger values of roughness z_o over the city. The increased surface roughness has the effect of increasing the rate of vertical transport and reducing the advective wind. There is very little evidence in these results of advective transport of dust from outside the city.

The rapid drop in vertical dust concentration for UTM Easting greater than around 418_{000} is notable. This drop is due to the rapid decrease in roughness, z_o, and to a decrease in local source strength; also increased deposition over the urban areas just to the west has decreased advective dust transport from these urban areas to the east of 418_{000}.

The effects on the vertical dust concentration profile of various model parameters can now be examined.

THE EFFECT OF ROUGHNESS, z_o, ON VERTICAL DUST CONCENTRATIONS

This, together with source strength, constitutes one of the decisive parameters in determining vertical concentration profiles. Its role has been indicated in the preceding discussion.

THE EFFECT OF DEPOSITION AND GRAVITATIONAL SEDIMENTATION ON VERTICAL DUST CONCENTRATIONS

This is shown clearly in Figs. 12 and 13. The expected effect of deposition and gravitational sedimentation is to lower the vertical dust concentrations above a certain height. This effect is more important over the urban areas with higher surface roughness and is more important for 20 μm particles.

THE EFFECT OF MEAN PARTICLE SIZE

Figs. 12 and 15 compare mean particle sizes of 5 μm and 20 μm, respectively. As would be expected, larger dust concentrations are found for 20 μm particles than for 5 μm particles below around 200 m. height, and smaller concentrations above 200 m. This effect of gravitational sedimentation is much more pronounced over the urban areas with higher surface

roughness, z_o, and hence larger rates of vertical transport. This leads also to an alteration in the isopleths as shown in Figs. 12 and 15.

THE EFFECT OF WIND SPEED ON VERTICAL DUST CONCENTRATIONS

In Figs. 15 and 16 the general forms of the isopleths are similar, the latter representing the assumption of twice the wind field of the former. For the higher wind field, the vertical dust concentrations are greater at all heights. This is because greater vertical transport rates are associated with higher wind speeds. With higher wind speeds, advective dust transport is important; this is shown downwind of the urban regions for UTM Easting greater than 418_{000}.

THE EFFECT OF TIME OF DAY ON VERTICAL DUST CONCENTRATIONS

In comparing Figs. 14 and 15 for 800 and 1100 LST, respectively, one sees a decisive difference in the isopleths over the urban area for these two cases. The 0800 case shows much less variation over the urban areas (398_{000} to 418_{000}) in the isopleths than for 1100. At 0800 the mixing height is small; this reduces the role of vertical transport. The advective winds for 0800 tend to "smooth" the isopleths over the urban area and produce somewhat greater uniformity at a given height. Also, at 0800 the sources have only recently been turned to their daytime values, and the dust concentrations aloft do not yet reflect the greatly increased day-time dust emission rates over the night-time values. By 1100 LST the mixing height approaches the maximum value and the increased day-time source emissions show up in the higher vertical dust concentrations.

SECTION 5

CONCLUSIONS

1. Observed high particulate concentrations in urban areas of Maricopa County during late fall and winter periods of atmospheric stability are associated with large local sources; because of the light drainage winds prevalent in late fall and winter in Maricopa County, the advective transport of dust from the countryside to the urban areas is not an important contribution to the urban dust loading.

2. Surface roughness and dry deposition, along with source strengths, are among the most important determinants of ground level particulate concentrations. Steps to reduce dust emissions in regions of high ambient particulate concentration would be one obvious remedy. Addition of trees and other foliage to increase surface roughness and deposition rates would also lower ground-level dust concentrations.

3. During late fall and winter periods of atmospheric stability, extremely large dust concentrations are found in a few areas where large local sources occur in conjunction with very low advective wind speeds. Paradise Valley is one example of such a situation.

Additional study is needed to perfect our particulate model of Maricopa County. The inadequacy of the available data prevent any quantitative, detailed test of our model. The available data were obtained by different investigators at different times and frequently with inadequate specification of meteorological conditions. Detailed knowledge of particle size distribution for the ambient aerosol and for the sources was lacking. However, results achieved with our current crude data base are encouraging. This leads to our view that an adequate and practical predictive model, along the lines suggested here, could be developed for Maricopa County as well as for the other urban areas in the high desert regions.

REFERENCES

1. Middleton, P. and Brock, J.R. Simulation of Aerosol Kinetics. J. Colloid and Interface Sci.

2. Suck, S.H., Middleton, P., and Brock, J.R. On the Multimodality of the Atmospheric Aerosol. Atmos. Environ. (In Press)

3. Middleton, P. and Brock, J.R. Modelling the Urban Aerosol. (To Appear.)

4. Brock, J.R. Processes, Sources and Size Distributions. In: Fogs and Smokes, Discussions of Faraday Society, London, 1974.

5. Lamb, R.G. 1973. Note on Application of K-Theory and Turbulent Diffusion Problems Involving Chemical Reaction. Atmos. Environ. 7:234.

6. Suck, S.H. and Brock, J.R. (To Appear.)

7. Shir, C.C. and Shieh, L.J. Development of Urban Air Quality Simulation Model with Compatible RAPS Data. Final Report, Contract 68-02-1833, IBM Research Laboratory, San Jose, California, May 1975.

8. TRW, Inc. Maricopa Co. Source Inventory, Personal Communication.

9. IITRI Report No. C633C05-2, Field Air Sampling Study. Phoenix, Arizona. April 1976.

10. Berman, N.S. and DeLaney, K.G. Atmospheric Modelling for Phoenix. Arizona Engineering Research Center Technical Report ERC-R-75009, May 1975.

11. U.S. Geological Survey, Map NI12-8, 1954.

12. U.S. Geological Survey, Map NI12-7, 1954 (Revised 1969).

13. Middleton, P. and Brock, J.R. Atmospheric Aerosol Dynamics: The Denver Brown Cloud. Denver Air Pollution Study - 1973, EPA Report EPA-600/9-76-007a, June 1976.